CANADIAN THESES ON MICROFICHE

THÈSES CANADIENNES SUR MICROFICHE

National Library of Canada
Collections Development Branch

Canadian Theses on
Microfiche Service

Ottawa, Canada
K1A 0N4

Bibliothèque nationale du Canada
Direction du développement des collections

Service des thèses canadiennes
sur microfiche

NOTICE

The quality of this microfiche is heavily dependent upon the quality of the original thesis submitted for microfilming. Every effort has been made to ensure the highest quality of reproduction possible.

If pages are missing, contact the university which granted the degree.

Some pages may have indistinct print especially if the original pages were typed with a poor typewriter ribbon or if the university sent us an inferior photocopy.

Previously copyrighted materials (journal articles, published tests, etc.) are not filmed.

Reproduction in full or in part of this film is governed by the Canadian Copyright Act, R.S.C. 1970, c. C-30. Please read the authorization forms which accompany this thesis.

AVIS

La qualité de cette microfiche dépend grandement de la qualité de la thèse soumise au microfilmage. Nous avons tout fait pour assurer une qualité supérieure de reproduction.

S'il manque des pages, veuillez communiquer avec l'université qui a conféré le grade.

La qualité d'impression de certaines pages peut laisser à désirer, surtout si les pages originales ont été dactylographiées à l'aide d'un ruban usé ou si l'université nous a fait parvenir une photocopie de qualité inférieure.

Les documents qui font déjà l'objet d'un droit d'auteur (articles de revue, examens publiés, etc.) ne sont pas microfilmés.

La reproduction, même partielle, de ce microfilm est soumise à la Loi canadienne sur le droit d'auteur, SRC 1970, c. C-30. Veuillez prendre connaissance des formules d'autorisation qui accompagnent cette thèse.

THIS DISSERTATION
HAS BEEN MICROFILMED
EXACTLY AS RECEIVED

LA THÈSE A ÉTÉ
MICROFILMÉE TELLE QUE
NOUS L'AVONS REÇUE

Canada

NL 339 (r. 86/09)

HYDROGEN ISOTOPE EXCHANGE WITH A WETPROOFED CATALYST

by

PAUL W.K. SETO

A thesis submitted to the School of Graduate Studies in partial fulfillment of the requirements for the degree of

MASTER OF APPLIED SCIENCE

in the

Department of Chemical Engineering

University of Ottawa

February, 1984

UNIVERSITÉ D'OTTAWA
UNIVERSITY OF OTTAWA

ABSTRACT

With the success of a newly developed wetproofed catalyst at AECL (Atomic Energy of Canada Limited), many new processes based on the catalytic isotopic exchange between hydrogen and liquid water have become feasible. The applications range from tritium recovery to heavy water production. With many potential applications, it is important to understand the behaviour and stability of the catalyst. In this work, catalyst activity and lifetime have been studied under various operating conditions.

The isotopic exchange between hydrogen gas and liquid water can be represented by two consecutive exchange steps:

$$HD_G + H_2O_V \overset{Pt}{\rightleftharpoons} H_{2_G} + HDO_V \qquad [1]$$

$$HDO_V + H_2O_L \rightleftharpoons H_2O_V + HDO_L \qquad [2]$$

Reaction [1] is a catalyzed exchange step and platinum has been found to be the best catalyst. The second reaction is a purely mass transfer step which can occur at any liquid-vapour interface. Thus, the overall exchange is the transfer of deuterium between hydrogen gas and liquid water and it can be carried out efficiently inside a trickle bed reactor.

The overall exchange process in a trickle bed reactor has been modelled in a global sense for the two reactions. With this model, the

influence of gas and liquid flow rates, total pressure and temperature on process performance have been assessed.

When the operating temperature was raised to 75°C, the activity of the catalyst was too low to warrant any further study. The loss in activity could be attributed to water condensation inside the pores of the catalyst, creating a diffusion barrier that effectively eliminates the fast gas reaction at the catalyst surface (i.e. reaction [1]).

To counteract the condensation of water, oxygen was injected into the gas stream in an attempt to keep the pores dry. This idea is based on the exothermic reaction between oxygen and hydrogen. Therefore, with a suitable amount of heat generated by this reaction, the pores inside the catalyst should not be plugged with condensed water. Results indicated that a stable catalyst activity was maintained with 500 ppm oxygen concentration in the inlet gas stream to the reactor.

Acknowledgement

I would like to express my sincere gratitude to my supervisor, Dr. K.T. Chuang for his patient and constant guidance throughout the course of this project.

My sincere appreciation also goes to Dr. D.D. McLean for his valuable suggestions.

Last, but not least, I am grateful to Mr. M.L. Coulas for his assistance in constructing the test facility and obtaining experimental data.

TABLE OF CONTENTS

PAGE

LIST OF FIGURES

LIST OF FIGURES continued...

NOMENCLATURE

G = superficial hydrogen gas flow rate, $mol.m^{-2}.s^{-1}$

L = superficial liquid water flow rate, $mol.m^{-2}.s^{-1}$

P = system total pressure, kPa

T = system temperature, °C

T_D = mass transfer rate between water vapour and liquid water, $mol.m^{-3}(bed).s^{-1}$

T_o = overall transfer rate between hydrogen gas and liquid water, $mol.m^{-3}(bed).s^{-1}$

T_R = catalytic exchange rate between hydrogen gas and water vapour, $mol.m^{-3}(bed).s^{-1}$

V = superficial water vapour flow rate, $mol.m^{-2}.s^{-1}$

x = deuterium atom fraction in liquid water

x_o = deuterium atom fraction in liquid water at bottom of reactor

y = deuterium atom fraction in hydrogen gas

y_E = deuterium atom fraction in hydrogen gas at the outlet of the high temperature equilibrator

y_o = deuterium atom fraction in hydrogen gas at bottom of reactor

α_D = separation factor between water vapour and liquid water

α_E = separation factor between hydrogen gas and water vapour at operating temperature of the high temperature equilibrator

α_R = separation factor between hydrogen gas and water vapour

α_o = separation factor between hydrogen gas and liquid water

ν = deuterium atom fraction in water vapour

ν_o = deuterium atom fraction in water vapour at bottom of reactor

ρk_R = catalytic transfer coefficient between hydrogen gas and water vapour, $mol.m^{-3}(bed).s^{-1}$

ρk_D = mass transfer coefficient between water vapour and liquid water, $mol.m^3(bed).s^{-1}$

$\Sigma K_y a$ = overall transfer coefficient between hydrogen gas and liquid water, $m^3(STP).s^{-1}.m^{-3}(bed)$

1. INTRODUCTION

1.1 Deuterium and heavy water

There are three known isotopes of hydrogen, namely,

protium (P) - the most abundant isotope commonly referred to as hydrogen (H) (atomic weight 1.0),

deuterium (D) - the second isotope of hydrogen with an atom fraction of about 150 ppm in natural water (atomic weight 2.0), and

tritium (T) - the radioactive isotope of hydrogen (atomic weight 3.0).

In isotope separation technology, the main interest is the change in concentration of the desired isotope in a given phase. Atom fraction (defined in 2.1) is commonly used to specify the total quantity of a particular isotope in a given phase. The advantage of using atom fraction is that there is no need to determine the form of the species that contain the desired isotope. For example, when hydrogen gas is enriched in deuterium, there exist different molecular species, namely H_2, HD and D_2. The deuterium atom fraction in this gas is the fraction of deuterium in the mixture. It provides no information on the distribution of deuterium among the three species. Nonetheless, for isotopic separation, it is adequate to know how much deuterium is in the gas regardless of the species that contain it.

Deuterium was first discovered by Urey and his co-workers at Columbia University in 1931 (1) and before long a relatively pure heavy

water was prepared by G.N. Lewis (2). Because of the special properties of deuterium and heavy water, they have become useful tools in many fields of research. For example, deuterium can be used as a tracer for hydrogen atoms in the field of biochemistry or as a source of deuterons which, when accelerated in a cyclotron, can cause a whole new set of phenomena, in the field of nuclear physics.

There are also many potential usages of heavy water, however, at the present state of the art, the principal use of heavy water is as a coolant and moderator in fission reactors, such as the CANDU nuclear reactor system.

Heavy water is one of the most important elements in the CANDU reactor. As a moderator, it enables the reactor to be fueled with natural uraniuim oxide because it absorbs neutrons much less readily. It also serves as a primary coolant to transport heat from the reactor core to a boiler filled with ordinary water which in turn is heated to generate steam. The steam is then used to drive a turbine which produces electricity. An excellent review of the CANDU reactor system is given in reference (3).

1.2 Hydrogen isotope separation

Among all of the isotopic separations, those involving hydrogen isotopes have an advantage over the others because of the high mass ratios indicated below:

Isotope Pair	Mass Ratio
T-H	3/1
D-H	2/1
T-D	3/2

These ratios are the highest found in the entire periodic table. It enhances both their physical and chemical differences. However, because of the small percentage of deuterium in nature, the production of heavy water is still very expensive.

Many ways of deuterium and heavy water production have been proposed; only a few are feasible for large scale production. A partial list of methods of separating heavy hydrogen or heavy water is given below (4):

1. Distillation of hydrogen
2. Hydrogen diffusion
3. Electrolysis of water
4. Distillation of water
5. H_2S-H_2O isotopic exchange (G-S process)
6. H_2-NH_3 isotopic exchange
7. H_2-H_2O isotopic exchange.

A comprehensive review of heavy water process development can be found in reference (5).

1.3 Hydrogen - water isotopic exchange

The current commercial process for making heavy water in Canada is based on the GS (Girdler-Sulphide) process which produces heavy water in two steps: the first being a bithermal exchange process between hydrogen sulphide gas and water (the most abundant source of deuterium on earth)

$$HDS + H_2O \rightleftharpoons H_2S + HDO \qquad [3]$$

and the second through water distillation. Although this process has been used to produce heavy water for many years, it suffers from a number of shortcomings including the necessity of dealing with the highly toxic and corrosive hydrogen sulphide gas at pressures of 2 MPa. Also, from an economic point of view, it becomes less and less favourable in a world of rising energy cost since it demands a very high energy consumption (30 GJ/kg D_2O) (5).

With the development of a novel wetproofed catalyst at AECL (Atomic Energy of Canada Limited), the catalytic exchange between hydrogen and liquid water emerges as the most promising alternative.

$$HD + H_2O \rightleftharpoons H_2 + HDO \qquad [4]$$

This new process possesses a number of inherent advantages, for example, the separation factor for the exchange between hydrogen and liquid water is about two times higher than the exchange between hydrogen sulphide and liquid water. As a result, theoretical recoveries as high as 50 percent are attainable for a bithermal process. From an energy requirement point of view, a bithermal exchange process demands

only one-quarter of the GS energy cost. This new scheme of heavy water production has been the subject of an intense research program at CRNL (Chalk River Nuclear Laboratories) for the last fourteen years.

In fact, Canada's first industrial heavy water plant operated from 1943 until 1956 at Trail, British Columbia was based on this exchange mechanism. The catalyst used was selected during the Manhattan Project (6). This Plant used electrolytic hydrogen enriched in deuterium. From this enriched hydrogen stream, deuterium was transferred to water vapour by a noble catalyst and from water vapour to liquid water in bubble cap trays. These two steps had to be carried out in a series of separated sections because the catalyst employed was deactivated by liquid water. Due to the complex multi-stage configuration, this process was not economically feasible for large scale heavy water production.

However, with the wetproofed catalyst which prevents water from coming into contact with the catalyst, the exchange can now be carried out efficiently in a trickle bed reactor in which hydrogen gas and liquid water flow countercurrently through a packed catalyst bed. This type of contacting scheme when operated monothermally is known as the LPCE (Liquid Phase Catalytic Exchange) process.

Hydrogen-water isotopic exchange with the wetproofed catalyst has been studied extensively in LPCE columns at around room temperature. Numerous papers on this subject have been published (7, 8, 9).

1.4 Tritium recovery from heavy water

One of the first applications of the wetproofed catalyst based on hydrogen-water isotopic exchange is the recovery of tritium from heavy water. Tritium is produced as a result of neutron absorption by deuterium atoms. Therefore, it is formed as a by-product in the heavy water cooled and moderated CANDU nuclear reactor. Its concentration in heavy water increases gradually with reactor operating time and since tritiated heavy water is radioactive, it constitutes a health hazard and thus an increase in maintenance cost.

The traditional way of removing tritium from heavy water is by vapour phase catalytic exchange (VPCE) in which tritium is transferred from heavy water to deuterium by means of a catalyst.

$$D_2 + DTO_v \overset{\text{catalyst}}{\rightleftharpoons} D_2O_v + DT \qquad [5]$$

As a result of the exchange step, the deuterium gas stream is diluted with both tritium and hydrogen which are then separated from deuterium by cryogenic distillation. This process requires the VPCE column to operate at 200°C to avoid catalyst deactivation by liquid water. Therefore, vaporization of the liquid feed is needed before catalytic exchange can take place. Also, the vaporized stream has to be condensed after the exchange. All these complicated evaporation and condensation steps (as shown in Figure 1) can be eliminated by adapting the wetproofed catalyst which can achieve the tritium transfer in a single catalyst column.

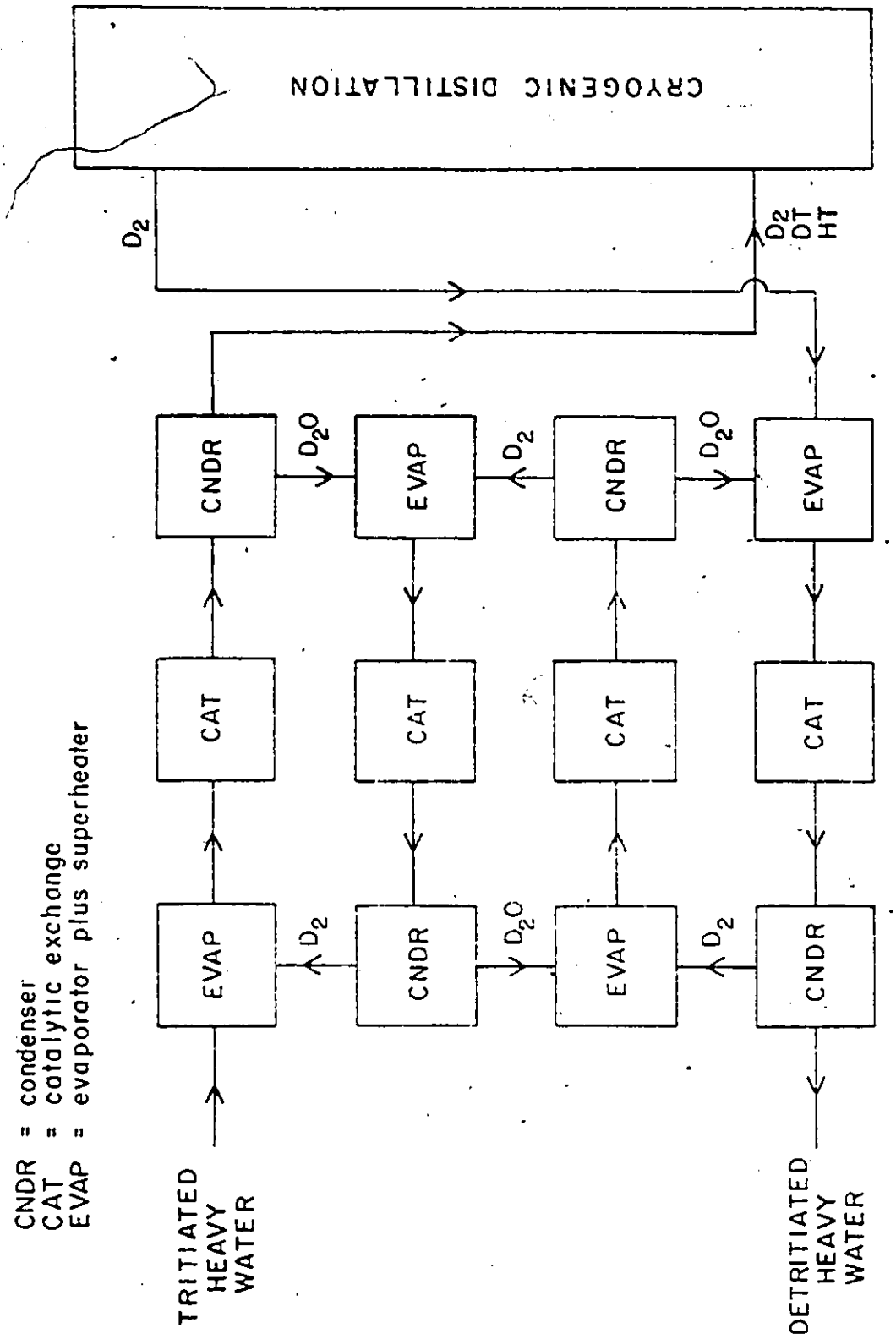

FIGURE 1 VPCE FLOWSHEET FOR DETRITIATION OF HEAVY WATER

A tritium extraction plant based on the LPCE process is being built at CRNL and is scheduled for completion in 1986. It consists of a LPCE front end where tritium is transferred from heavy water into the recirculating deuterium gas and a cryogenic distillation unit which separates tritium from deuterium. A simplified flowsheet of the extraction plant is shown in Figure 2.

The use of high temperatures are preferred for tritium recovery from heavy water because tritium concentrates more in the gas phase as the temperature rises. Therefore, there is a need to know the behaviour of wetproofed catalyst at temperatures up to the normal boiling point of water.

1.5 Objectives of this work

Although the wetproofed catalyst has been demonstrated to have long and stable activity at temperatures up to 60°C (10), it is of interest to know the catalyst performance at even higher temperatures where the water vapour pressure is considerably higher.

Temperature (°C)	Vapour Pressure Increase Relative to 25°C
25	1.0
60	6.3
75	12.2
90	22.1

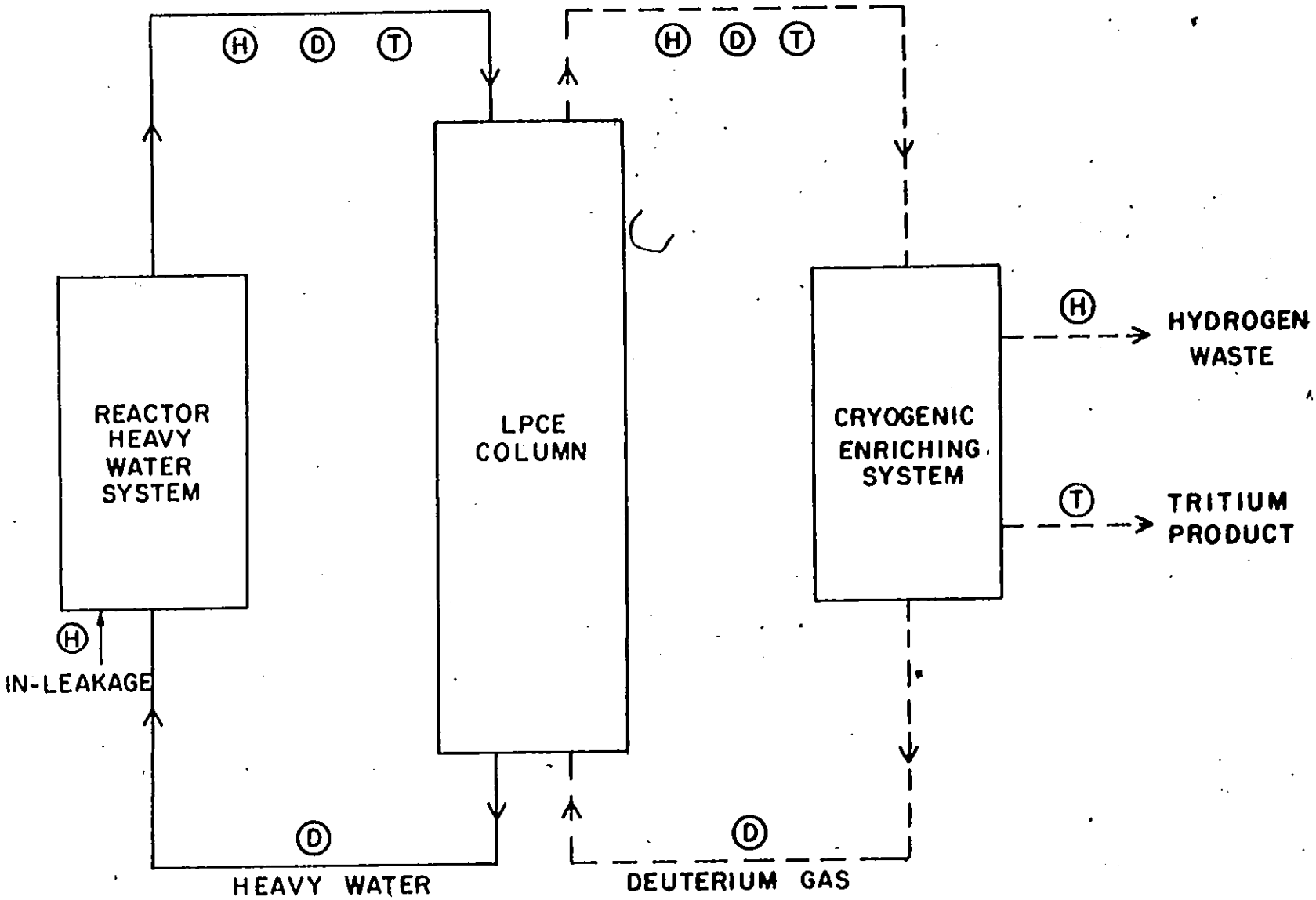

FIGURE 2 A SIMPLIFIED TRITIUM EXTRACTION PLANT FLOWSHEET

At higher water vapour pressures, it is possible that capillary condensation inside the catalyst pores will become significant, therefore causing an excessive loss in catalyst activity.

In the event of unacceptable catalyst activity at higher temperatures, oxygen will be injected into the system. This idea was first proposed by Chuang (11) and had been found to be successful in maintaining high and stable catalyst activity by Japanese researchers (12) for their catalysts. The principle is based on the fact that the reaction between oxygen and hydrogen is exothermic (ΔH_{298} = -484 kJ/mole) and with a suitable amount of heat generated, it should be able to keep the catalyst pores free of condensate.

There are two main objectives in this work:

1. To measure the performance and stability of the wetproofed catalyst at various temperatures.

2. To investigate the influence of oxygen injection when pore condensation at high temperatures becomes significant.

The results of this work will provide information on the temperature limit of the wetproofed catalyst which will be taken into consideration in the design of the CRNL tritium extraction plant. As the isotope exchange between tritium and deuterium has the same mechanism as the exchange between deuterium and hydrogen, the latter

was used to reduce construction complications and operational hazards.

2. THEORETICAL BACKGROUND

2.1 Atom fraction

It is customary to express composition in a mixture of two isotopes in terms of the atom fraction of the desired isotope. Atom fraction is defined as the ratio of the number of atoms of desired isotope of an element to the total number of atoms of the element.

2.2 Separation factor

The separation factor for isotopic exchange processes can be determined by the usual static or dynamic equilibration methods (13). It is defined as the ratio of desired component in the phase in which it concentrates divided by the ratio of desired component in the other phase.

In the case of hydrogen-water isotopic exchange, the separation factor, α_R, for the exchange between water vapour and hydrogen gas is given by,

$$\alpha_R = \frac{\nu^*/(1-\nu^*)}{y^*/(1-y^*)} \qquad [6]$$

where ν^* - equilibrium deuterium atom fraction in vapour

y^* - equilibrium deuterium atom fraction in gas.

For the separation between liquid water and water vapour, the separation factor α_D is given by,

$$\alpha_D = \frac{x^*/(1-x^*)}{v^*/(1-v^*)} \qquad [7]$$

where x^* - equilibrium deuterium atom fraction in liquid.

Finally, for the overall separation between liquid water and hydrogen gas, the overall separation factor α_o is given by,

$$\alpha_o = \frac{x^*/(1-x^*)}{y^*/(1-y^*)} \qquad [8]$$

2.3 Transfer mechanism

The protium-deuterium transfer in hydrogen-water isotopic exchange involves the following reactions,

$$H_2O + D_2 \rightleftharpoons HDO + HD \qquad [9]$$

$$HDO + D \rightleftharpoons D_2O + HD \qquad [10]$$

$$HDO + HD \rightleftharpoons D_2O + H_2 \qquad [11]$$

$$H_2O + HD \rightleftharpoons HDO + H_2 \qquad [12]$$

However, when deuterium concentrations are in the ppm level, one can assume there are practically no D_2O and D_2 molecules (see Figures 3 and 4), therefore only reaction [12] occurs. Basically, reaction [12] can be divided into two consecutive steps.

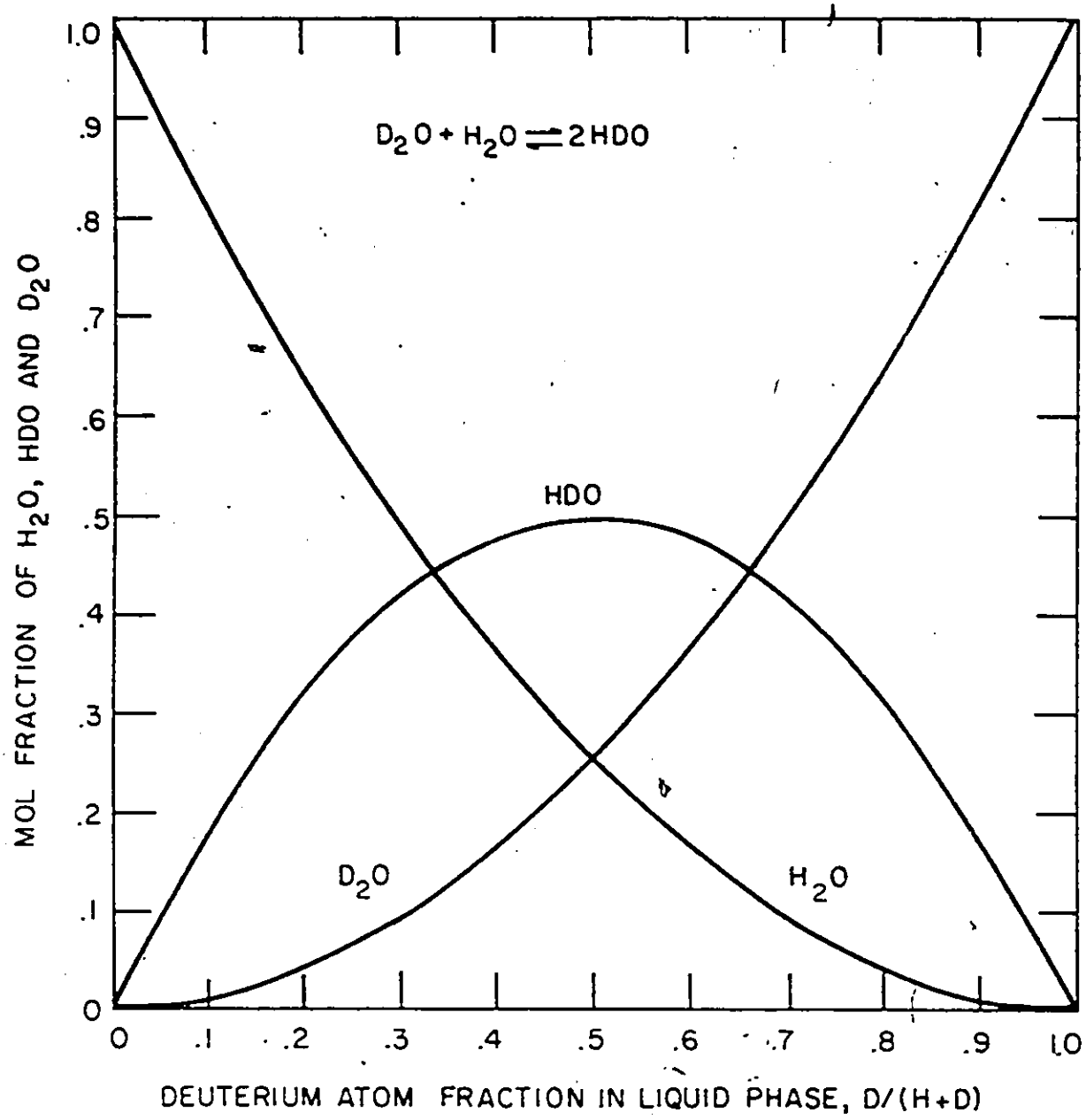

FIGURE 3 EQUILIBRIUM CONCENTRATIONS OF D_2O, HDO AND H_2O AT 25°C

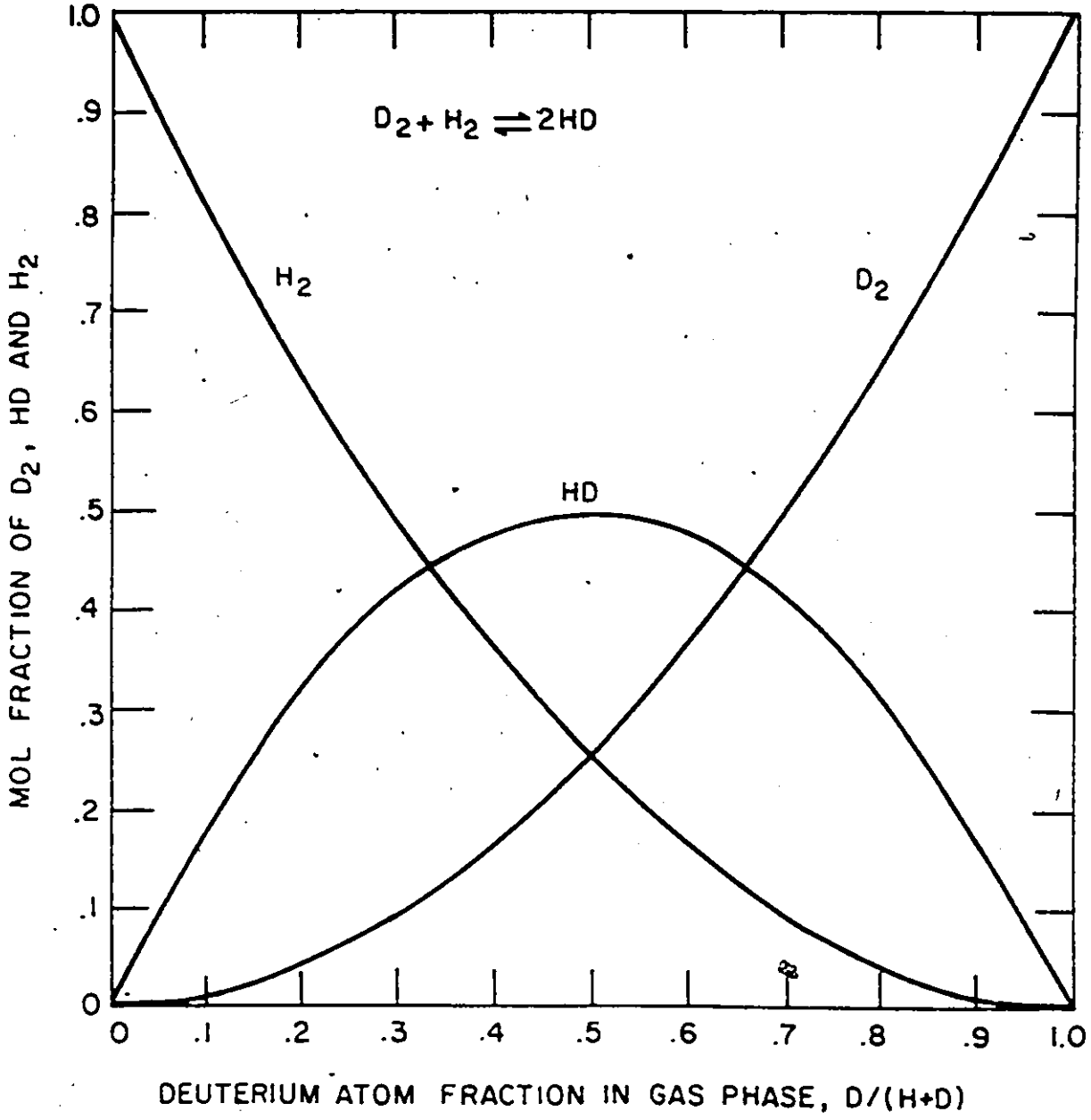

FIGURE 4 EQUILIBRIUM CONCENTRATIONS OF D_2, HD AND H_2 AT 25 °C

$$HD_G + H_2O_V \overset{Pt}{\rightleftharpoons} H_{2_G} + HDO_V \qquad [13]$$

$$HDO_V + H_2O_L \rightleftharpoons H_2O_v + HDO_L \qquad [14]$$

The first step is the catalytic exchange step and the reaction is given by [13]. This is a gas phase reaction and is catalyzed by platinum which transfers the deuterium between hydrogen gas and water vapour. The second step is a pure mass transfer step and can be described by [14]. In this step, deuterium is transferred between water vapour and liquid water and this can take place at any vapour-liquid interface.

2.4 Process model

The process model is based on the LPCE configuration. The assumptions involved in this model are that:

1. isothermal bimolecular reversible processes are involved in both catalytic reaction [13] and mass transfer [14],

2. plug flow prevails in both gas and liquid phases,

3. negligible direct transfer occurs between hydrogen gas and liquid water.

With these assumptions, one can write the deuterium mass balance on an infinitesimal column element for liquid, vapour, and gas flow

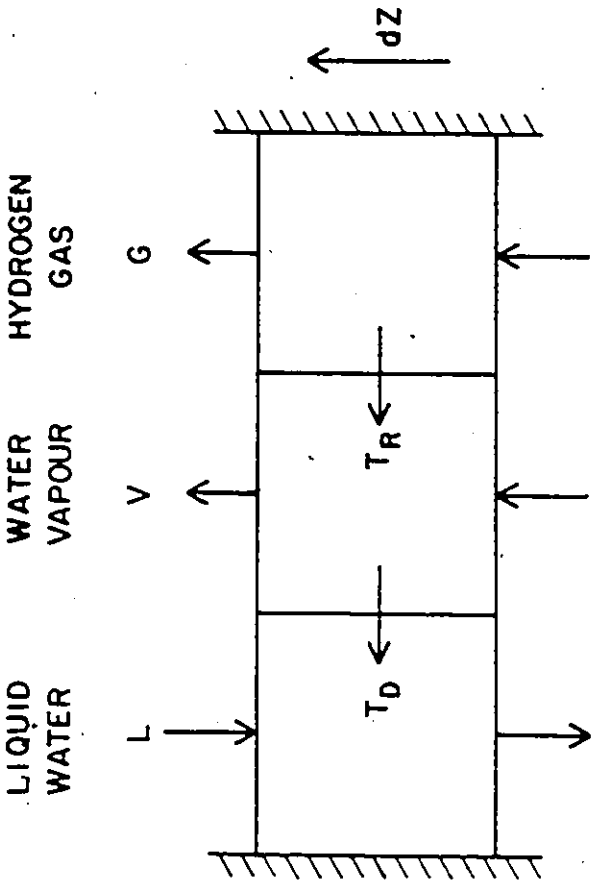

FIGURE 5 AN INFINITESIMAL COLUMN ELEMENT IN A TRICKLE BED REACTOR

(Figure 5), resulting in three differential equations (see 8.1), as follows:

Gas Stream $$-G \frac{dy}{dz} = \rho k_R[\alpha_R y(1-\nu) - \nu(1-y)] \quad [15]$$

Vapour Stream $$V \frac{d\nu}{dz} = -G \frac{dy}{dz} + L \frac{dx}{dz} \quad [16]$$

Liquid Stream $$-L \frac{dx}{dz} = \rho k_D[\alpha_D \nu(1-x) - x(1-\nu)] \quad [17]$$

Equation [15] is the deuterium mass balance on gas stream while equation [16] and [17] are for the vapour and liquid flow, respectively. Under low deuterium concentration, i.e. when x, ν and y $\ll 1$, [15] and [17] can be simplified to

$$-G \frac{dy}{dz} \simeq \rho k_R(\alpha_R y - \nu) \quad [18]$$

and

$$-L \frac{dx}{dz} \simeq \rho k_D(\alpha_D \nu - x) \quad [19]$$

Equations [16], [18] and [19] can be solved analytically to give the concentration profiles of deuterium in all three streams along a trickle bed reactor and the solution (14) is given by equation [20], [21] and [22], respectively.

$$y = A + B \text{ EXP } (-f_1 \rho k_R Z/G) + C \text{ EXP } (-f_2 \rho k_R Z/G) \quad [20]$$

$$\nu = \alpha_R A + (\alpha_R - f_1) B \text{ EXP } (-f_1 \rho k_R Z/G) + (\alpha_R - f_2) C \text{ EXP } (-f_2 \rho k_R Z/G) \quad [21]$$

$$x = \alpha_R \alpha_D A + (V/L)(\alpha_R + (G/V) - f_1) B \text{ EXP } (-f_1 \rho k_R Z/G) + (V/L)(\alpha_R + (G/V) - f_2) C \text{ EXP } (-f_2 \rho k_R Z/G) \quad [22]$$

where

$$A = \frac{\gamma}{\alpha_R - \gamma} \frac{LX_o - Gy_o - V\nu_o}{G}$$

$$B = \frac{-f_2\gamma}{(f_1-f_2)(\alpha_R-\gamma)} \frac{L}{G} (\alpha_D\nu_o - x_o) + \frac{\alpha_R-\gamma-f_2}{(f_1-f_2)(\alpha_R-\gamma)} (\alpha_R y_o - \nu_o)$$

$$C = \frac{f_1\gamma}{(f_1-f_2)(\alpha_R-\gamma)} \frac{L}{G} (\alpha_D\nu_o - x_o) + \frac{f_1-(\alpha_R-\gamma)}{(f_1-f_2)(\alpha_R-\gamma)} (\alpha_R y_o - \nu_o)$$

$$f_1 = \frac{1}{2} \left[\alpha_R + \frac{G}{V}\left(1+\frac{\phi}{\gamma}\right)\right] \left(1+\sqrt{1-Q}\right)$$

$$f_2 = \frac{1}{2} \left[\alpha_R + \frac{G}{V}\left(1+\frac{\phi}{\gamma}\right)\right] \left(1-\sqrt{1-Q}\right)$$

$$Q = \frac{4(G/V)(\phi/\gamma)(\alpha_R-\gamma)}{\left[\alpha_R+(G/V)(1+\phi/\gamma)\right]^2}$$

$$\phi = \frac{\rho k_D}{\rho k_R} \frac{G}{L}$$

$$\gamma = \frac{G}{(L\alpha_D - V)}$$

The profiles along a trickle bed reactor based on equations [20], [21] and [22] have been verified experimentally (17), thus supporting the validity of this model.

A typical profile was simulated based on equations [20], [21] and [22] (Figure 6). The enriched gas comes in at the bottom of the reactor and is slowly depleted of its deuterium content as it rises through the column. The countercurrent liquid stream comes in at the top and becomes enriched in deuterium as it trickles down through the reactor. As for the vapour stream, it comes in at equilibrium with the exit liquid at the bottom of the reactor.

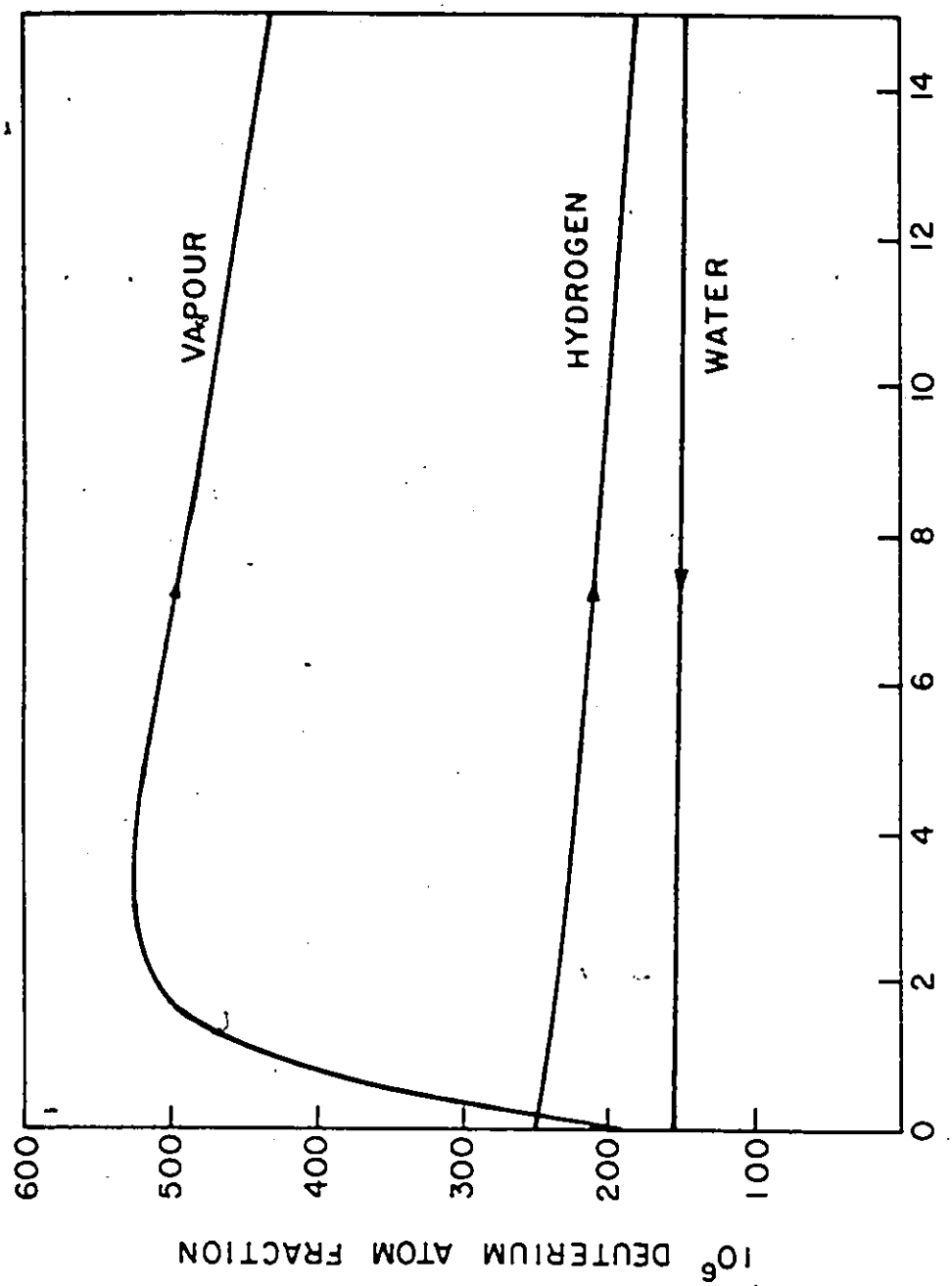

FIGURE 6 DEUTERIUM CONCENTRATION PROFILES IN A TRICKLE BED REACTOR

Due to a large driving force, its deuterium concentration increases rapidly toward the equilibrium with hydrogen gas.

The exit concentration for the vapour stream at the top of the reactor depends on the relative magnitude of the two transfer coefficients ρk_R and ρk_D. However, the exit concentration will lie somewhere between the gas-vapour equilibrium and the vapour-liquid equilibrium.

2.5 Data treatment

Basically, the exchange process is characterized in a global sense by two transfer coefficients. For example, the catalytic transfer coefficient, ρk_R, represents a complex combination of several simultaneous phenomena, namely, the diffusion of reactants and products through the external stagnant film, the diffusion and reaction inside the catalyst pores. On the other hand, the mass transfer coefficient, ρk_D, describes the transfer of HDO between the bulk of gas phase and the bulk of liquid phase.

In order to extract the experimental value of ρk_R and ρk_D, it is necessary to obtain the inlet and outlet concentrations of the gas, vapour, and liquid streams. Hence, altogether a total of six deuterium concentration measurements are required. However, based on the fact that natural water has a constant deuterium concentration of 144 ppm at CRNL and the imposed experimental condition of equilibrium between exit

liquid water and entering vapour, the required concentration measurements can be reduced to three, namely, the inlet and outlet deuterium concentration of the gas stream as well as vapour deuterium concentration at the top of the reactor. With all the concentration values and flow rates, we can then calculate the experimental values of ρk_R and ρk_D from the following equations (14).

$$\Delta_R = \alpha_R{}^{y-\nu} \quad [23]$$

$$\Delta_D = \alpha_D{}^{\nu-x} \quad [24]$$

$$\gamma = G/(L\alpha_D - V) \quad [25]$$

$$R = (f_1 - f_2)\ B\ \mathrm{EXP}(-f_1 \lambda Z) \quad [26]$$

$$f_1 = 0.5\ [\alpha_R + (G/V)(1+\phi/\gamma)](1+\sqrt{1-Q}) \quad [27]$$

$$f_2 = 0.5\ [\alpha_R + (G/V)(1+\phi/\gamma)](1-\sqrt{1-Q}) \quad [28]$$

$$Q = [4(G/V)(\phi/\gamma)(\alpha_R - \gamma)]/[\alpha_R + (G/V)(1+\phi/\gamma)^2 \quad [29]$$

$$B = \frac{-f_2\ \gamma}{(f_1-f_2)(\alpha_R-\gamma)} \frac{L}{G} (\alpha_D y_o - x_o) + \frac{\alpha_R - \gamma - f_2}{(f_1-f_2)(\alpha_R-\gamma)} (\alpha_R y_o - \nu_o) \quad [30]$$

$$\phi = \frac{\Delta_R - R}{\Delta_D + (G/\gamma L)R} \left\{ \frac{G+V\alpha_R}{L} - \frac{GV(\alpha_R-\gamma)}{L^2\gamma} \frac{\Delta_R - R}{\Delta_D + (G/\gamma L)\Delta_R} \right\} \quad [31]$$

$$\lambda = \frac{1}{f_2 z} \ln \frac{f_1(\gamma L/G)\Delta_{Do} + (f_1 - \alpha_R + \gamma)\Delta_{Ro}}{(f_1-f_2)[(\gamma L/G)\Delta_D + \Delta_R] - (\alpha_R - \gamma)R} \quad [32]$$

$$\rho k_R = \gamma G \quad [33]$$

$$\rho k_D = \phi\ \lambda L \quad [34]$$

A computer program has been written based on these equations to calculate ρk_R and ρk_D (Appendix 8.2).

The overall effect can be seen by combining the two transfer coefficients together to form an overall transfer coefficient called $\Sigma K_y a$ which is defined by:

$$-F \frac{dy}{dz} = \Sigma K_y a \, (y-y^*) \qquad [35]$$

where

F - superficial linear gas velocity ($m.s^{-1}$)

y^* - deuterium concentration of hydrogen gas in equilibrium with liquid water.

It can be shown that the relation between $\Sigma K_y a$, ρk_R and ρk_D is given by

$$\frac{1}{\Sigma K_y a} = \frac{44.617}{\alpha_o + x(1-\alpha_o)} \left[\frac{\alpha_D + x(1-\alpha_D)}{\rho k_R} + \frac{1+y(\alpha_R-1)}{\rho k_D} \right] \qquad [36]$$

The derivation of [36] can be found in Appendix 8.3.

3. EXPERIMENTAL

3.1 Wetpoofed catalysts

Conventional catalysts used for hydrogen-water isotopic exchange are hydrophilic. They are easily deactivated by liquid water.

Therefore, liquid water has to be vapourized before contacting the catalysts. Accompanying the vapourization process is the increase in water vapour pressure which causes significant capillary condensation inside the pores of the catalyst thus poisoning the catalyst. This necessitates the superheating of the vapourized stream in order to keep the pores dry.

The complicated vapourization and superheating stages can be eliminated with the employment of wetproofed catalyst. It was first invented by Stevens (15) and has been further developed at CRNL. Its applications have recently been reviewed by Seddon et al. (16). The difference between a wetproofed or so called hydrophobic catalyst as opposed to a hydrophilic catalyst is shown in Figure 7. It can be seen that there is a sac of air surrounding the hydrophobic catalysts while the ordinary catalysts are soaked with water. The ability of wetproofed catalyst to repel liquid water enables the gaseous reactants and products to diffuse readily to, and from, the active catalyst sites. Therefore, they are capable of achieving reaction rates comparable to those for conventional hydrophilic catalysts operating in dry environments.

At present, many techniques of producing hydrophobic catalyst have been found and detailed preparation methods have been documented in several proprietary AECL reports. The wetproofed catalyst used in this study was in the form of a sphere and prepared by the AECL Dip Method. Basically, the wetproofed catalyst consists of black platinized carbon powder mixed with Teflon which acts both as a binder and a wetproofing

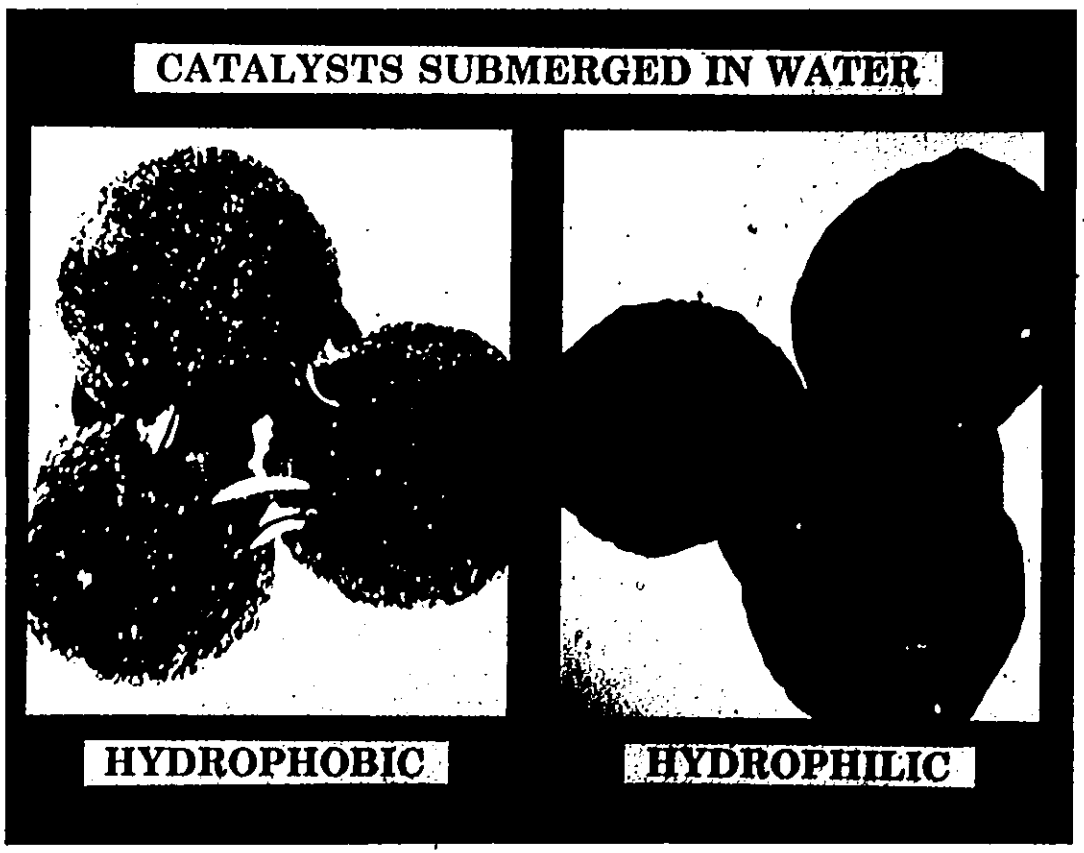

FIGURE 7: Hydrophobic and Hydrophilic Catalysts

agent. This mixture is then deposited as a thin layer on an inert ceramic sphere which acts as a support. The diameter of the catalyst was about 7 mm.

To characterize this particular batch of catalyst, the total surface area (BET area) and platinum metal area were determined by nitrogen adsorption and hydrogen chemisorption, respectively using the Accusorb model 2100E surface area analyser. The determined values were

BET area - 2.677 m^2/g of catalyst metal area - 0.203 m^2/g of catalyst

3.2 Reactor

The hydrogen-water isotopic exchange process was carried out in a trickle bed reactor where liquid water trickled down through the column countercurrent to hydrogen gas saturated with water vapour. It is well known that the performance of trickle bed reactors can be influenced by many factors. One major factor relevant to this study is the liquid distribution which has a direct impact on the vapour-liquid mass transfer rate.

As mentioned in the discussion of the isotope exchange mechanism, the isotope transfer between hydrogen gas and liquid water takes place indirectly by means of water vapour. Therefore, if the mass transfer rate between liquid water and water vapour is small relative to the catalytic exchange rate between water vapour and hydrogen gas, the

overall transfer will be small giving rise to an inefficient use of the catalyst bed. For example, it has been shown that a 100 percent hydrophobic catalyst bed gave lower performance than a catalyst bed diluted to 50 percent by volume with hydrophilic inert spheres of the same size (9). This is concievably caused by the maldistribution of water inside the 100 percent hydrophobic catalyst bed. Therefore, a 50:50 (by weight) mixed bed was employed in this study to alleviate the channelling effect inside the 50 mm diameter column. The bed height for this work was chosen to be 0.4 m.

In conventional rate measurements, an inert section containing packing of similar size to the catalyst is usually placed on top and bottom of the catalyst bed to establish flow patterns. In this work no inert section was placed on top of the mixed catalyst bed because this would promote the vapour-liquid transfer and thus distort the rate measurements. However, a mockup dye test in a glass column revealed that liquid flow profile developed within 2 cm from the top of the mixed bed when a 5-point liquid distributor was employed. Since the total bed height was 0.4 m the error in rate determination was not expected to be significant.

3.3 Test facility description

A simplified flow sheet of the test rig is shown in Figure 8. All equipment in contact with process water and gas was constructed from 304 stainless steel. The test rig built was based on the once-through-water/recirculating-gas principle.

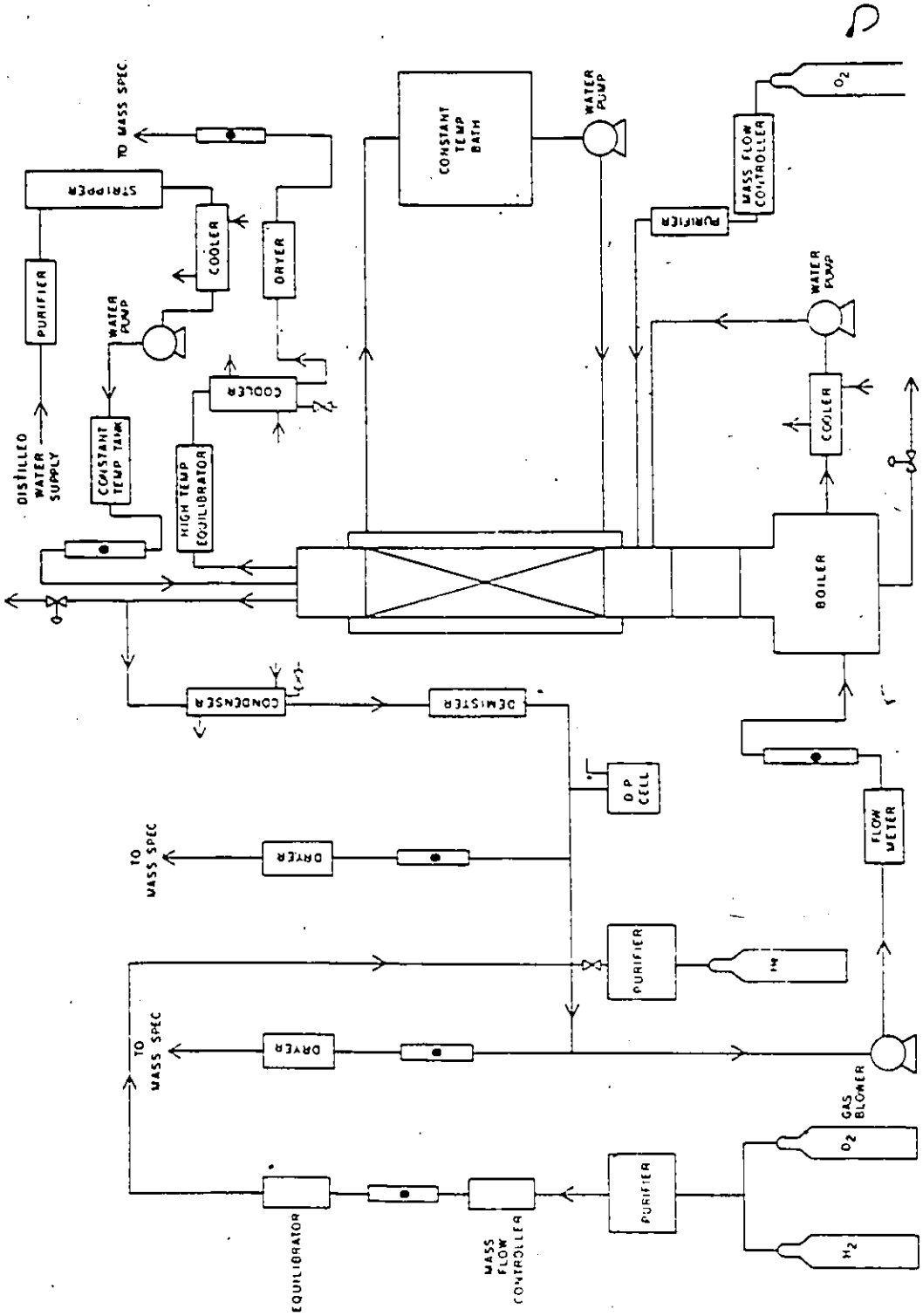

FIGURE 8 A SIMPLIFIED SCHEMATIC DIAGRAM OF TEST RIG

Distilled water was purified and deionized to about 10^{-10} ohm-cm by a Millipore Purification System (model ZD30-000-70) prior to entering the stripper where dissolved gases were stripped off by steam. The liquid water feed was then brought to the operating temperature by passing it through a constant temperature bath. Flow rate was measured with a rotameter ahead of the reactor and controlled manually by adjusting a needle valve at the rotameter outlet. Liquid water was fed into the reactor through a 5-point liquid distributor. It then trickled down the catalyst bed by gravity and collected in the boiler where the water level was maintained by a Foxboro liquid level controller (model 40).

Hydrogen gas was recirculated by means of a welded-bellows compressor (Metal Bellows Corporation, model MB-602) which delivered hydrogen gas to the boiler. The flow was monitored continuously by a precalibrated Tylan mass flow meter (model FM-362-35). A variac controlled 3 kW electrical heater was used in the boiler to heat and humidify the gas at the same time. The hot gas was brought to the desired temperature in a 0.5 m Goodloe Packing section by spraying water at the operating temperature. Temperature and humidity of the upflowing gas was monitored continuously by a Vaisala probe (Vaisala Inc. Model HMH-14UTA). The saturated gas then entered an equilibration section consisting of 0.1 m of Dixon ring packing followed by 0.05 m of ceramic spheres. This section ensured the vapour to be in isotopic equilibrium with the liquid water leaving the bottom of the reactor. The reactor was packed with wetproofed sphere catalysts diluted to 50% by weight with hydrophilic spheres of the same size. The gas and vapour

mixture from the top of the reactor passed through a condenser and a York mesh demister before returning to the compressor thus completing the cycle.

Make up (ordinary) and spiking (enriched) hydrogen gas were introduced to the gas loop through a Matheson Hydrogen Purifier (Johnson-Matthey model 8372) in which hydrogen diffused through a Pd-Ag alloy tube. The flow rate of the purified gas was controlled by a Tylan mass flow controller (model FC260-45) which led the gas into an equilibration section packed with 0.3 m of wetproofed catalyst. This section was designed to bring the hydrogen and deuterium gas into isotopic equilibrium.

$$H_2 + D_2 \rightleftharpoons 2HD \qquad [37]$$

When oxygen was required, it was injected into the gas stream at the bottom of the reactor equilibration section. The flow rate was also controlled by a mass flow controller (model FC-260).

A water jacket surrounding the reactor was used to maintain a constant reactor temperature. The temperature of the recirculating water through the water jacket was controlled by a Fenwal temperature controller (model 55-004420-302).

As mentioned in Section 2.5, three deuterium concentration measurements were required in each run. It was relatively easy to obtain deuterium concentration in the gas stream by on-line mass

spectrometer analysis (see section 3.5). As for the deuterium concentration in the vapour stream, it was much more convenient to use Butler's indirect method (17). This method involved the use of a 0.025 m diameter high temperature equilibrator filled with wetproofed sphere catalyst to a depth of 0.1 m. The equilibrator was wrapped with heating tape which had a variac-controlled power supply to maintain the operating temperature at around 150°C. The purpose of the equilibrator was to bring the gas and vapour mixture at the top of the reactor to isotopic equilibrium. Then from the gas equilibrium value, one can back calculate the deuterium concentration in the vapour at the top of the reactor by a simple mass balance,

$$\mathcal{V}_T = \frac{y_E\,(1 + \alpha_E\, V/G) - y_T}{V/G} \quad , \qquad [38]$$

This relationship is a valid approximation for low deuterium levels (17).

A photograph of the test assembly is given in Figure 9.

3.4 Test procedure

At the beginning of each test run, the recirculating gas and once through liquid water in every point of the reactor were at equilibrium. The spiking technique was used to upset this equilibrium and thus enabled the transfer rate to be measured. The procedure involved the continuous injection of a small hydrogen gas stream at high deuterium

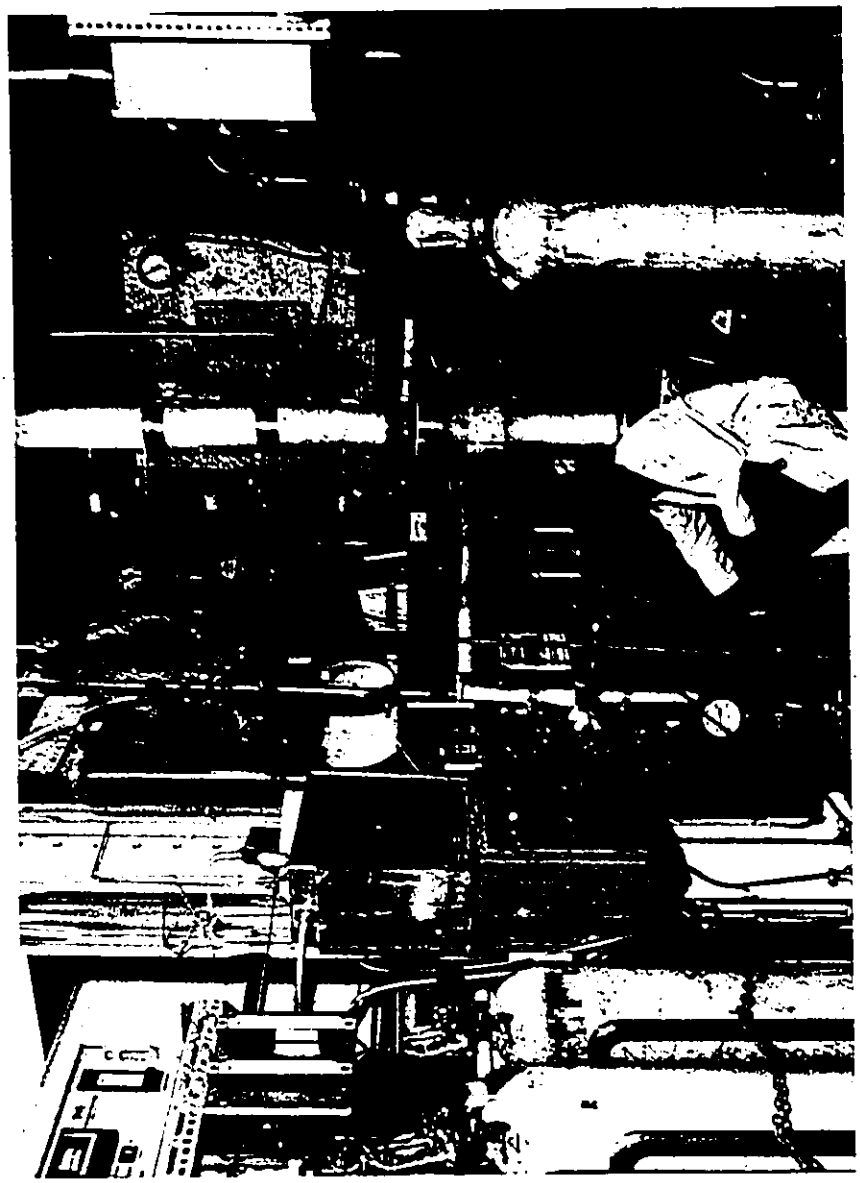

Figure 9: A photograph of the test assembly

atom fraction into the gas loop which disturbed the equilibrium between gas and liquid. It took about two hours for the test rig to reach a new steady state condition in which the inlet and outlet deuterium concentrations of all three streams from the reactor were constant with time. After all the necessary concentration measurements were made by on-line mass spectrometer, the results were then fed into a computer for performance analysis.

3.5 Deuterium concentration determination

Density, mass and infrared spectra are the three principal ways for measuring deuterium concentrations in hydrogen gas and water. However, when concentration is at the ppm level, the most convenient and accurate method of measuring deuterium concentration is by mass spectrometry. Mass spectrometry is capable of giving directly the concentration of different isotope species in samples by detecting the relative abundance of ions of mass 2 (hydrogen) and 3 (deuterium). The layout of the mass spectrometer (Associated Electrical Industry MS-20) used in this work is shown schematically in Figure 10.

Basically, the mass spectrometer assembly consisted of the following systems:

1. Sample inlet system - a stainless steel inlet system incorporating three crimp valves which operates at a reduced pressure. These

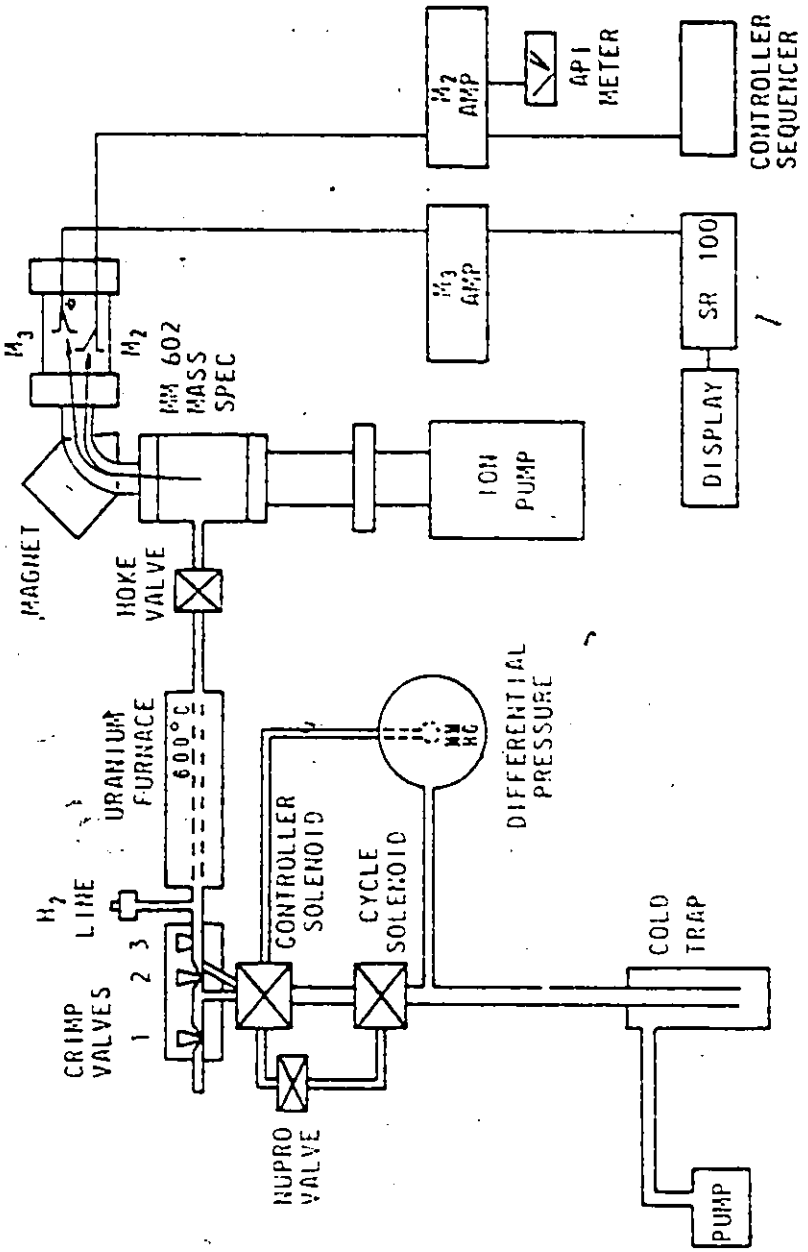

FIGURE 10. A simplified schematic diagram of the mass spectrometer

valves are designed to permit the controlled introduction of hydrogen to the mass spectrometer tube unit.

2. Spectrometer tube unit - two signals representing the hydrogen and deuterium are generated in this unit and read by two separate Cary electrometers.

3. Vacuum systems - three vacuum systems are connected to one another to provide pressure in the order of 10^{-9} Pa in the tube unit.

4. Electronic control and amplifier units - this set up ensures the production of strong and stable hydrogen and deuterium signals.

5. Digital voltmeter and printer - this unit translates the signals from the electronic circuit into deuterium concentration in ppm.

A detailed description and operation procedure is given in reference (18). The mass spectrometer used in this study had an accuracy of $\pm$ 1 ppm.

4. Results and discussions

4.1 Comparison of catalyst performance at 25°C

An initial experiment was conducted to determine if the catalyst was consistent in activity and stability with others studied at CRNL under similar conditions.

After 30 days of operation, a steady state overall transfer coefficient of 0.76 s^{-1} was obtained at a hydrogen flow rate of 0.82 $m.s^{-1}$ (STP). The performance of the catalyst was evaluated at various hydrogen flow rates so that comparison with similar catalysts could be carried out. From Figure 11, it can be seen that the present catalyst has a higher activity than the one tested in the 62 mm LPCE test rig. It has been shown that catalyst with higher platinum loading gives higher activity (19). Therefore, the enhanced activity observed for the present catalyst is probably due to the higher platinum loading of the present catalyst (0.38 wt% vs 0.21 wt%). Since this new batch of catalyst has the same order of magnitude of activity as the one measured in the 62 mm LPCE rig, it was concluded that the present catalyst was representative of the wetproofed catalysts under examination by CRNL.

4.2 Effect of operating variables on the catalytic transfer coefficient at 60°C

After performance tests at 25°C had been completed, the temperature of the column was raised to 60°C. This phase of the work was undertaken to measure reactor performance at high temperatures under various operating conditions. The effects of liquid flow, gas flow and total pressure on the process were studied since they are the primary variables with which engineers can manipulate for the design and operation of a large industrial plant.

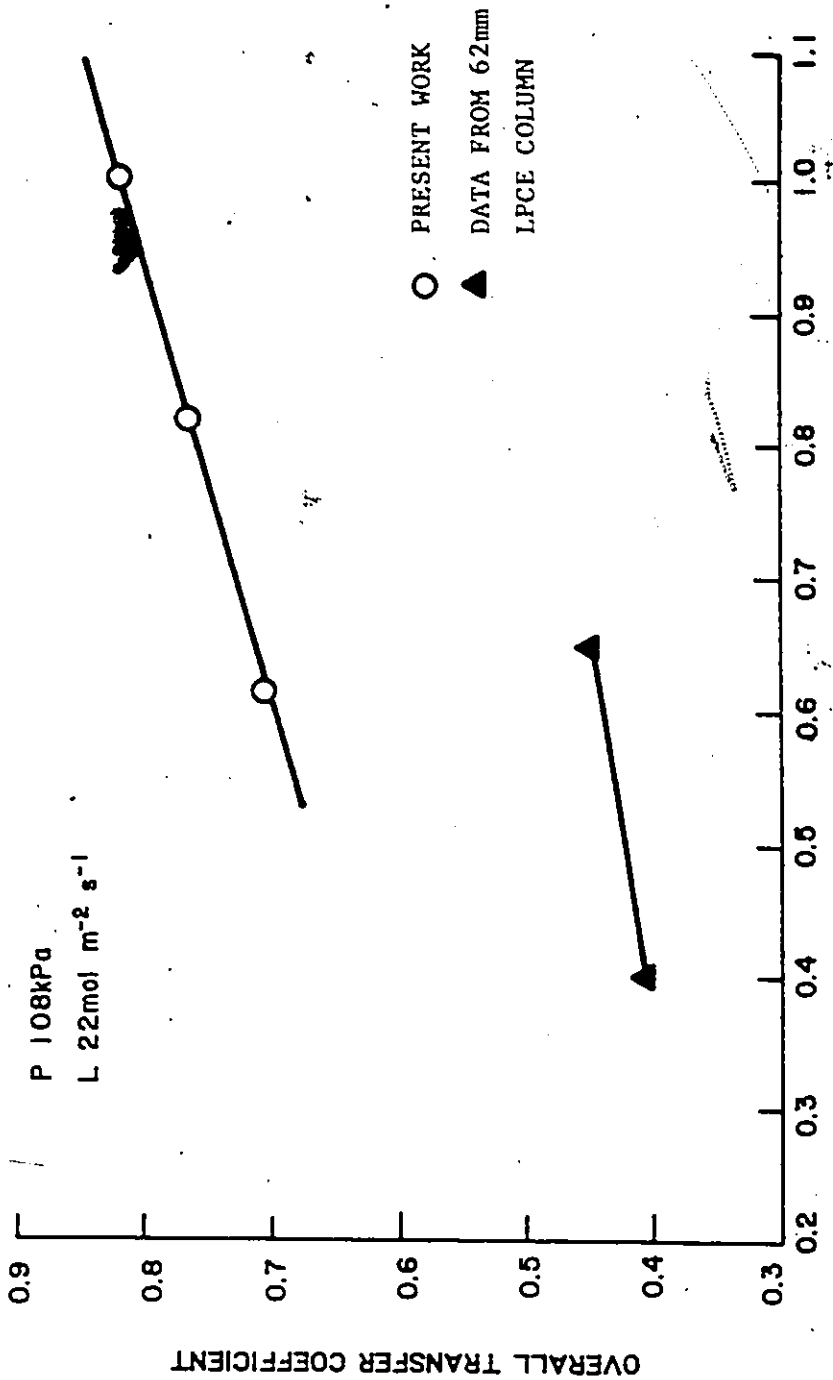

FIGURE 11 DEPENDENCY OF OVERALL TRANSFER COEFFICIENT ON HYDROGEN GAS VELOCITY AT 25°c

It is important that all performance tests be conducted at a steady catalytic activity. As can be seen from Figure 12, the catalyst activity in terms of the overall transfer coefficient, $\Sigma K_y a$, stayed relatively constant during the entire testing period.

In Figures 13, 14 and 15, the effects of total pressure, gas and liquid flow rate on vapour-gas catalytic transfer coefficient, ρk_R are illustrated, respectively. The dominant feature in these figures is the relatively large increase in ρk_R as the gas flow is raised from 0.6 to 1 $m.s^{-1}$ (STP). This suggests that the gas phase transfer process is not free from external diffusion resistance through the gas-solid boundary layer. On the other hand, both total pressure and liquid flow rate have a negative correlation with ρk_R. The decrease in transfer rate with increasing total pressure is anticipated because of lower diffusion coefficient at higher pressure. The drop in ρk_R with higher liquid flow is likely because of more water trickling over the hydrophobic surface therefore effectively blocking the entrance of the catalyst pores. Similar observations were also reported by Enright and Chuang (20).

4.3 Dependency of operating variables on mass transfer coefficient at 60°C

Figures 16, 17 and 18 show the effects of total pressure, gas and liquid flow rate on the vapour-liquid mass transfer coefficient ρk_D, respectively. It can be seen that ρk_D is strongly influenced by the

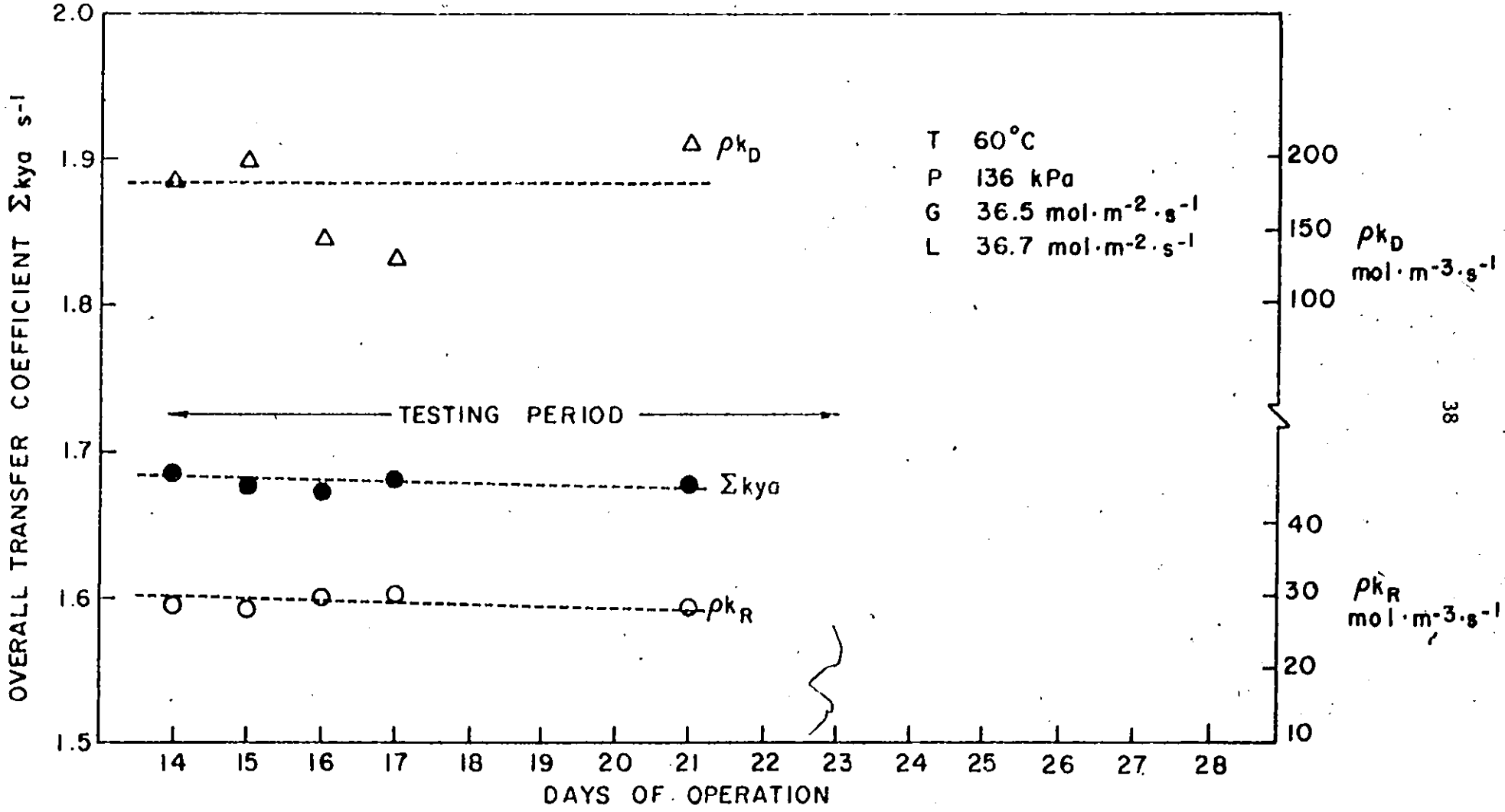

FIGURE 12 STABILITY OF CATALYST ACTIVITY DURING TEST PERIOD AT 60C

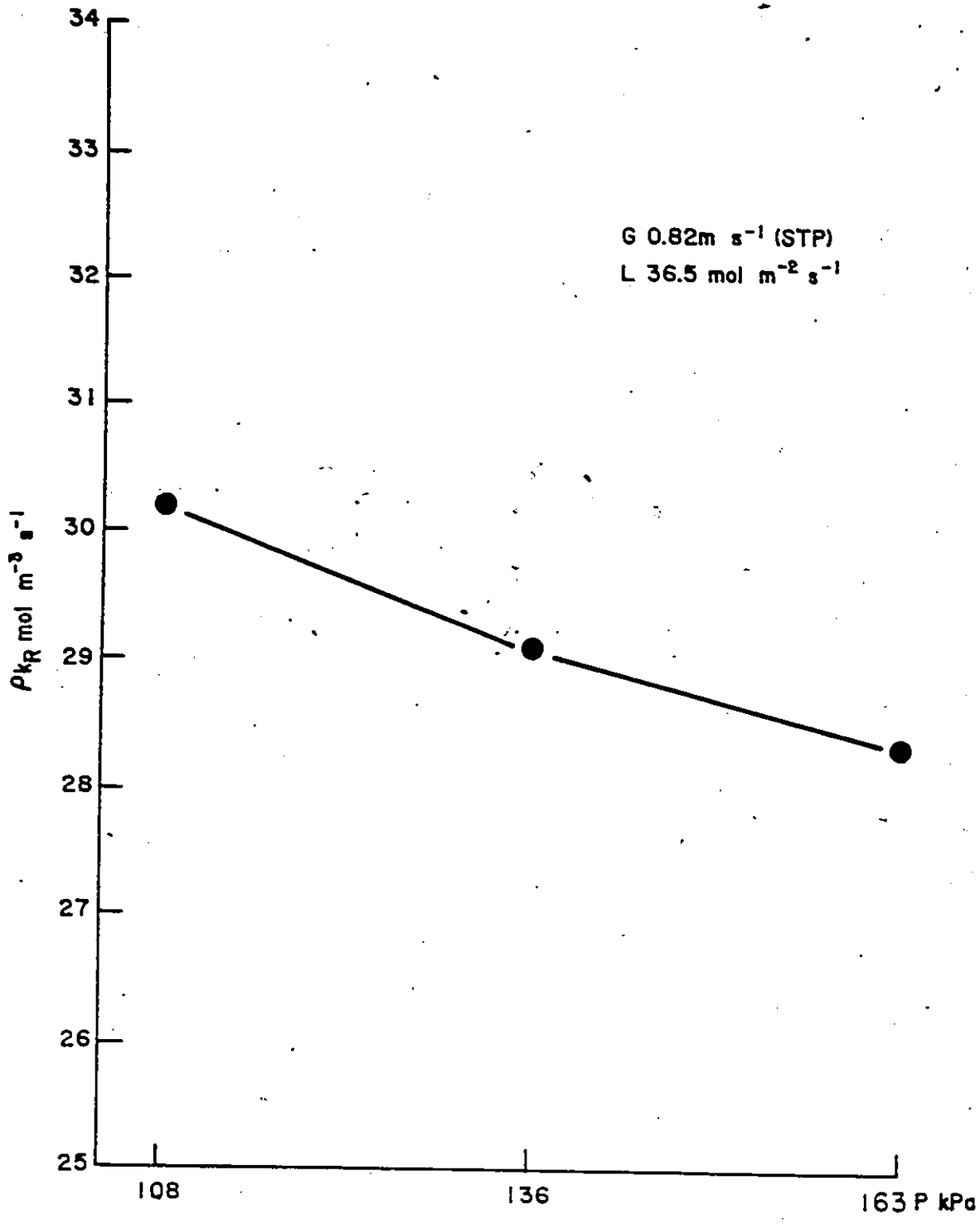

FIGURE 13 EFFECTS OF SYSTEM PRESSURE ON ρk_R AT 60°C

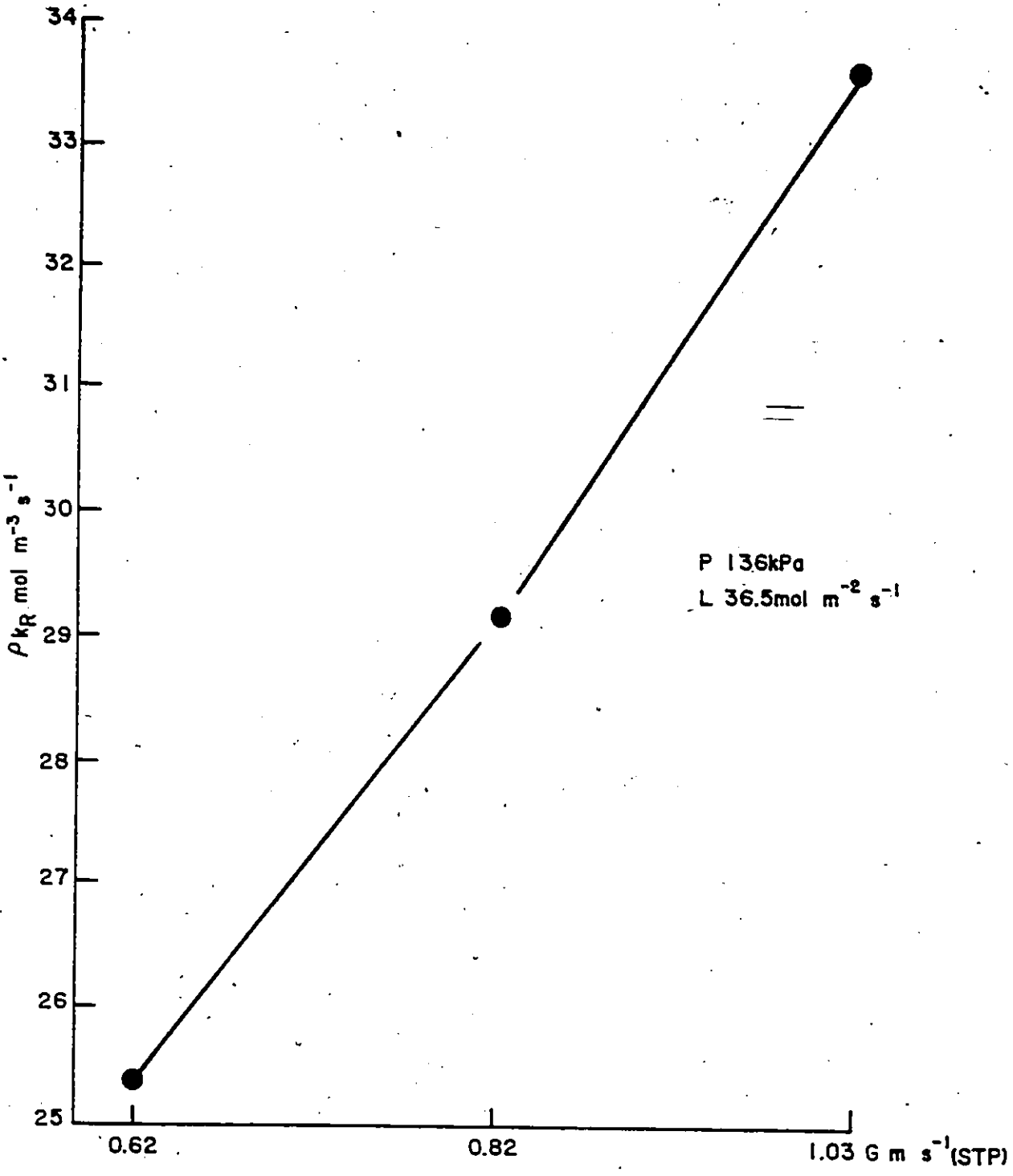

FIGURE 14 EFFECTS OF GAS FLOW ON ρk_R AT 60°C

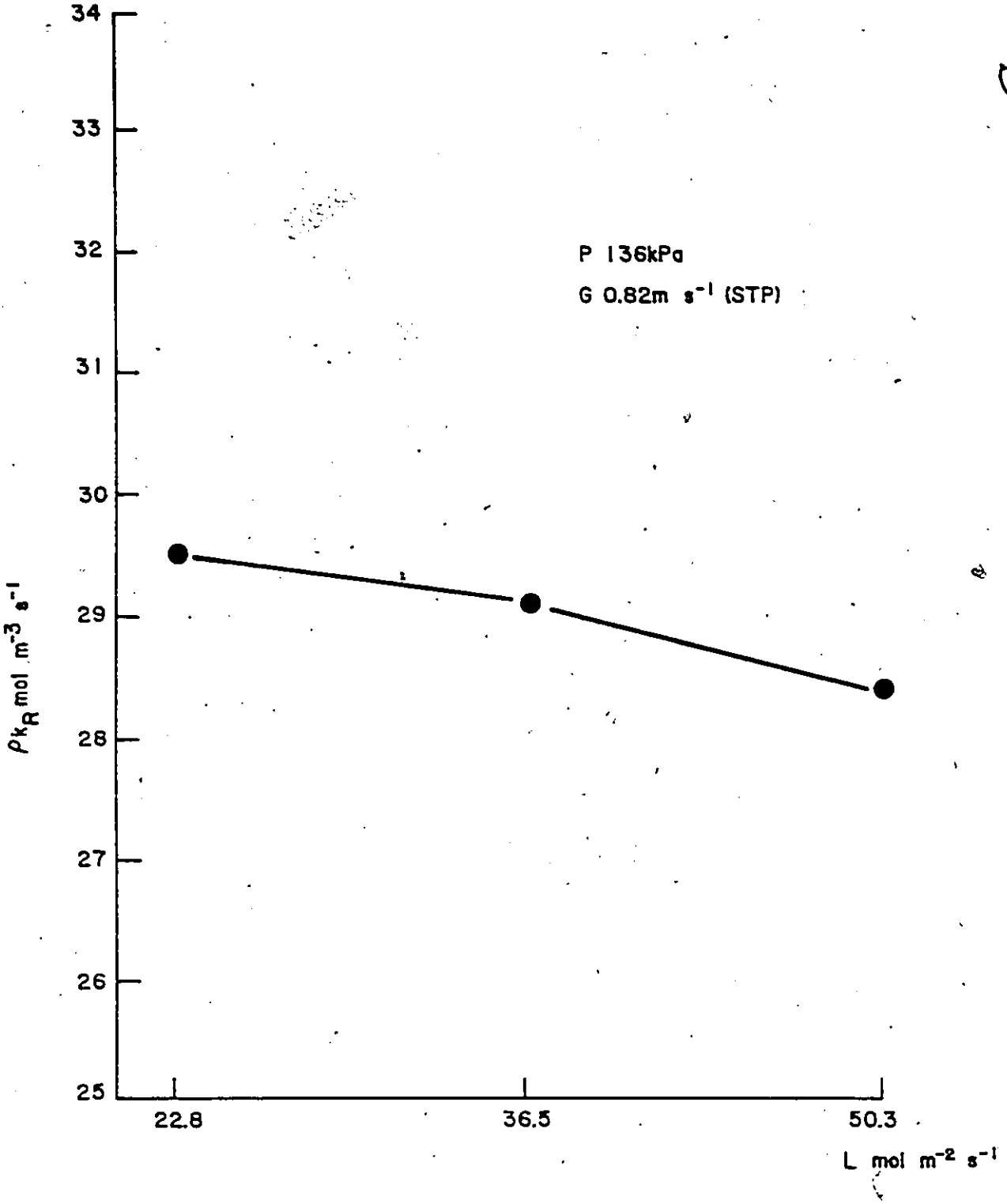

FIGURE 15 EFFECTS OF LIQUID FLOW RATE ON ρk_R AT 60°C

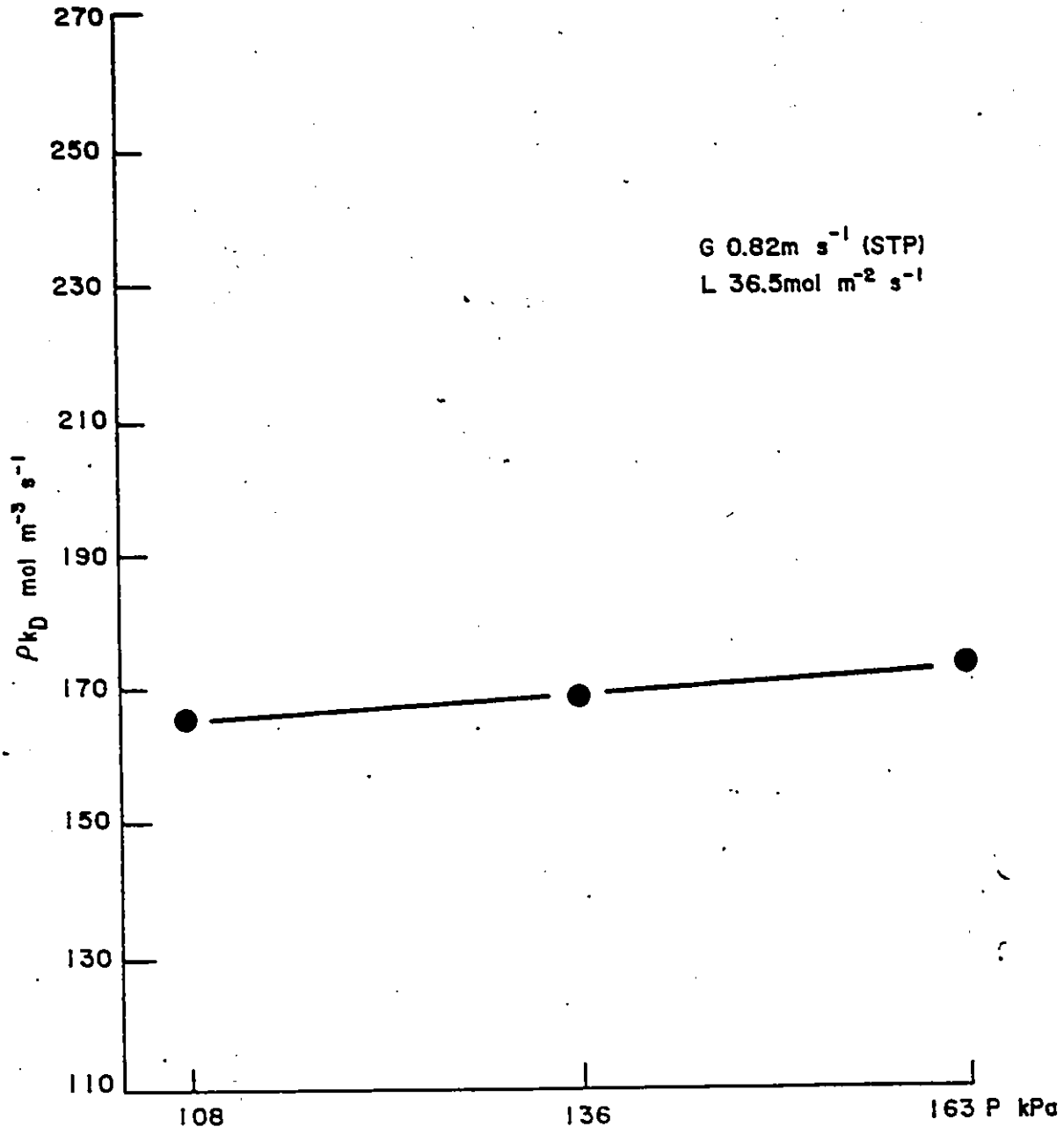

FIGURE 16 EFFECTS OF SYSTEM PRESSURE ON ρk_D AT 60°C

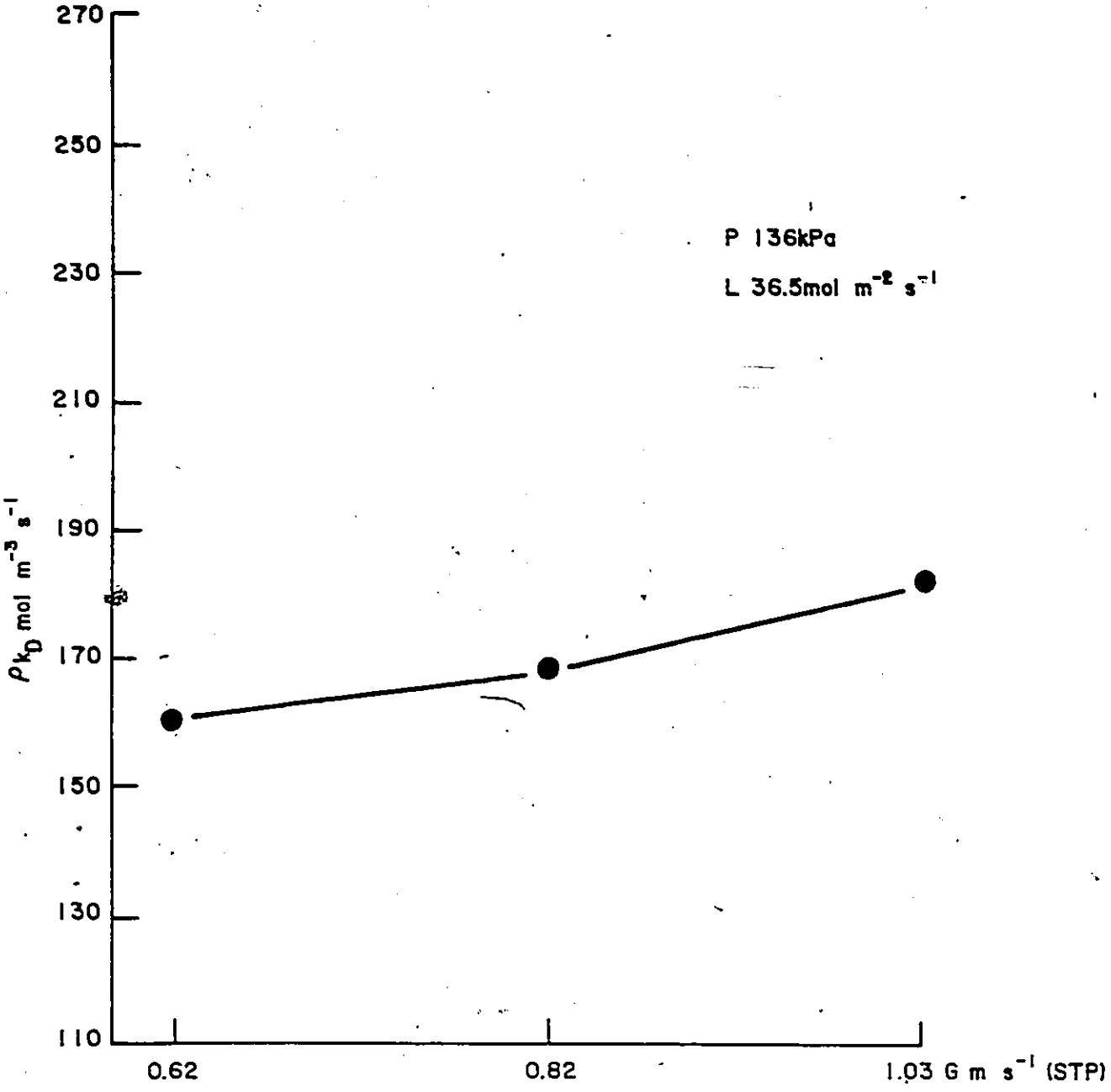

FIGURE 17 EFFECTS OF GAS FLOW RATE ON ρk_D AT 60°C

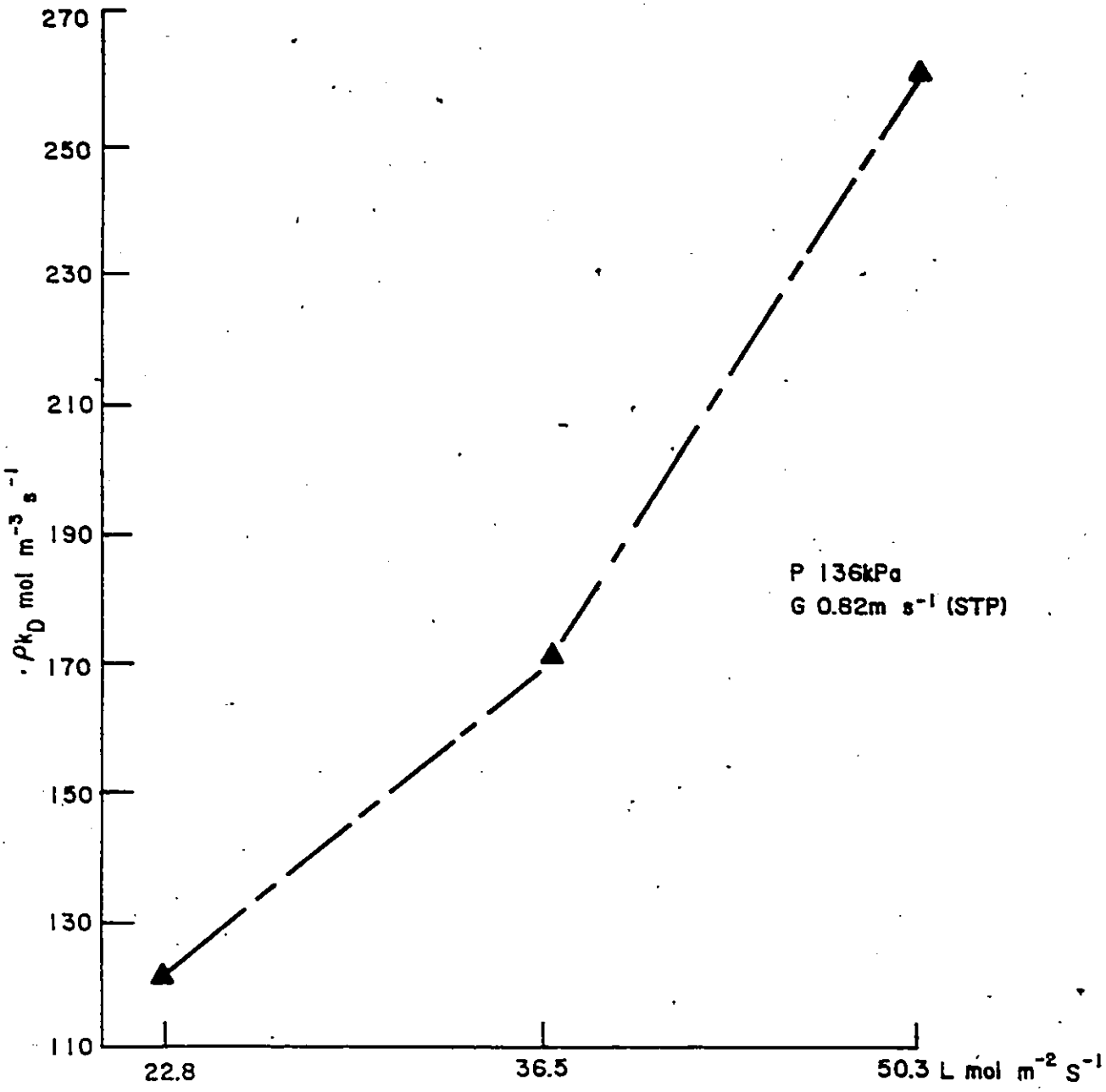

FIGURE 18 EFFECTS OF LIQUID FLOW RATE ON ρk_D AT 60°C

liquid flow rate which reinforces the notion that ρk_D characterizes the transfer between liquid water and water vapour. Within the tested liquid flow rate range, ρk_D rises with liquid flow rate. This can be attributed to the increase in the effective vapour-liquid mass transfer area. Increase in gas flow rate and total pressure also resulted in a smaller increase in the ρk_D value. The former enhancement can be explained in terms of the decrease in thickness of the stagnant film at the vapour-liquid interface. However, it is not expected that ρk_D to increase with increasing pressure. Since vapour-liquid transfer is a molecular diffusion process and molecular diffusion coefficient is inversely proportional to total pressure, therefore ρk_D should decrease with rising pressure. The observed increase in ρk_D (8 $mol.m^{-3}.s^{-1}$) is within the scattering (standard deviation = 10 $mol.m^{-3}.s^{-1}$) of the experimental ρk_D value. Hence, any conclusion is of questionable validity.

4.4 Influence of operating variables on the overall transfer coefficient at 60°C

The combined effects of the two transfer steps in hydrogen-water isotope exchange can be examined by plotting $\Sigma K_y a$ (the overall transfer coefficient) versus the testing variables. From Figures 19, 20 and 21, it can be concluded that, within the testing range, an increase in both gas and liquid flow rate will enhance the overall performance of the process but gas flow rate has a larger influence on $\Sigma K_y a$ than liquid flow rate. On the other hand, it was observed that there was a slight drop in $\Sigma K_y a$ as the pressure of the system was raised from 108 to 163 kPa.

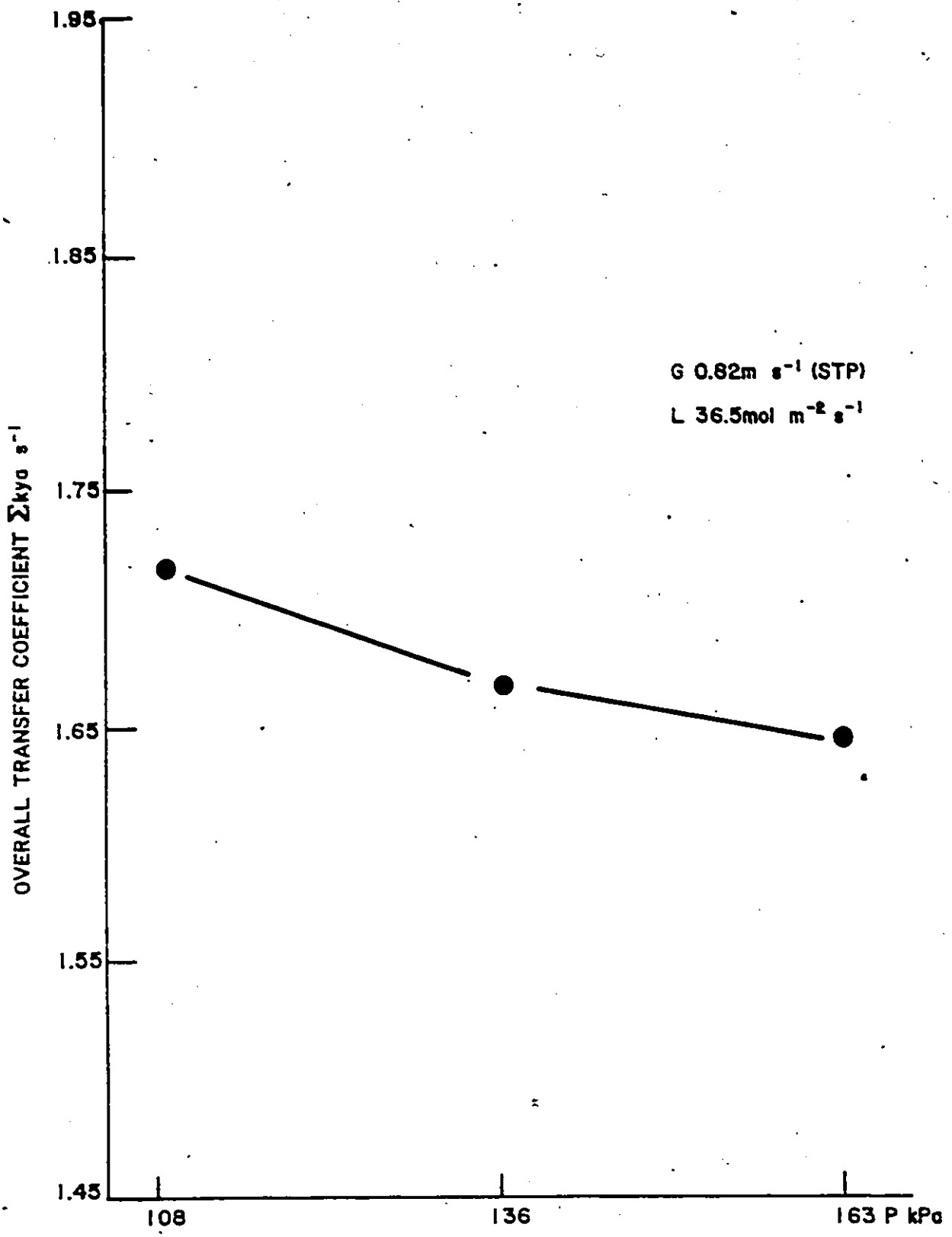

FIGURE 19 EFFECTS OF SYSTEM PRESSURE ON $\Sigma k_y a$ AT 60°C

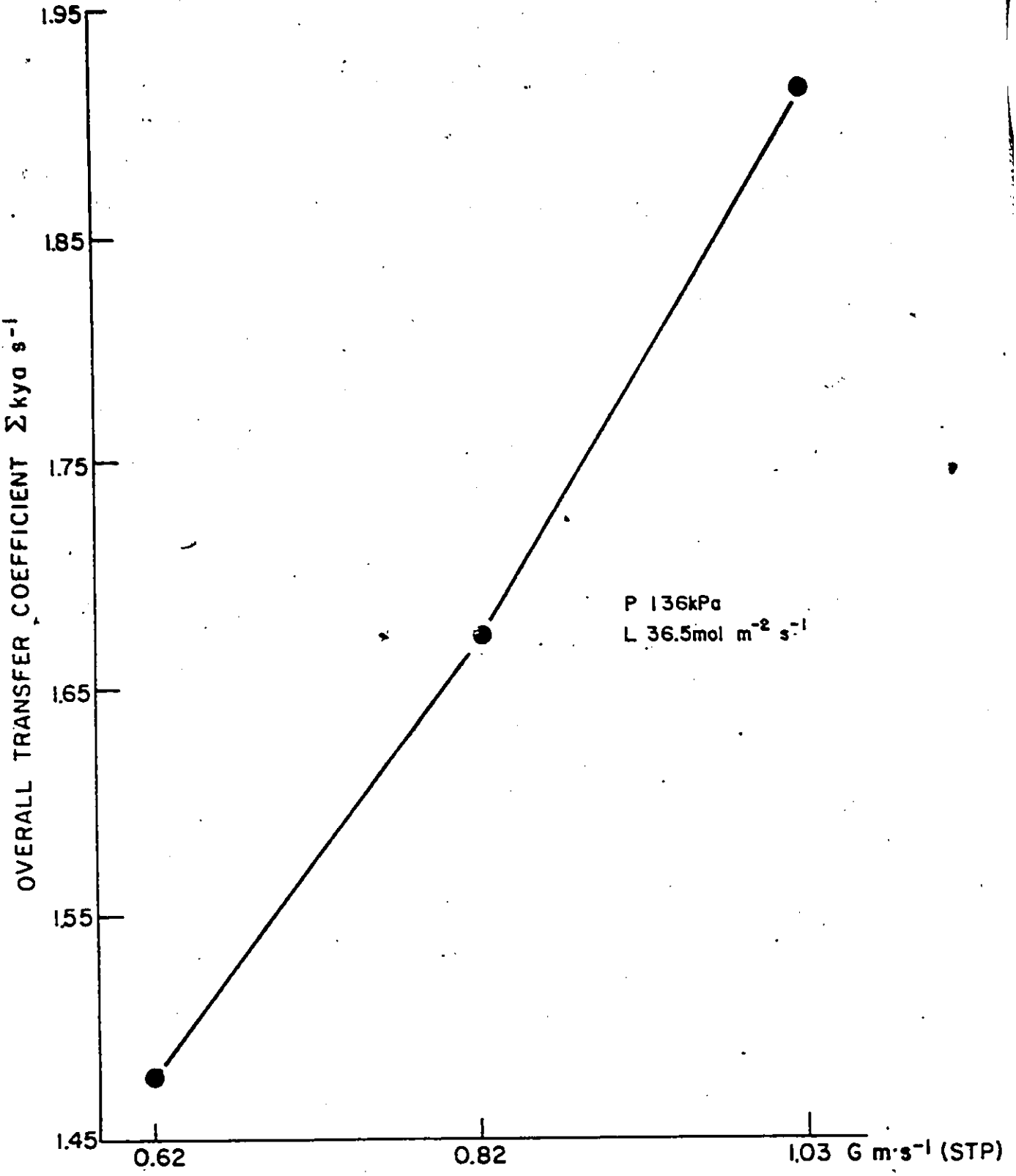

FIGURE 20 EFFECTS OF GAS FLOW RATE ON Σkya AT 60°C

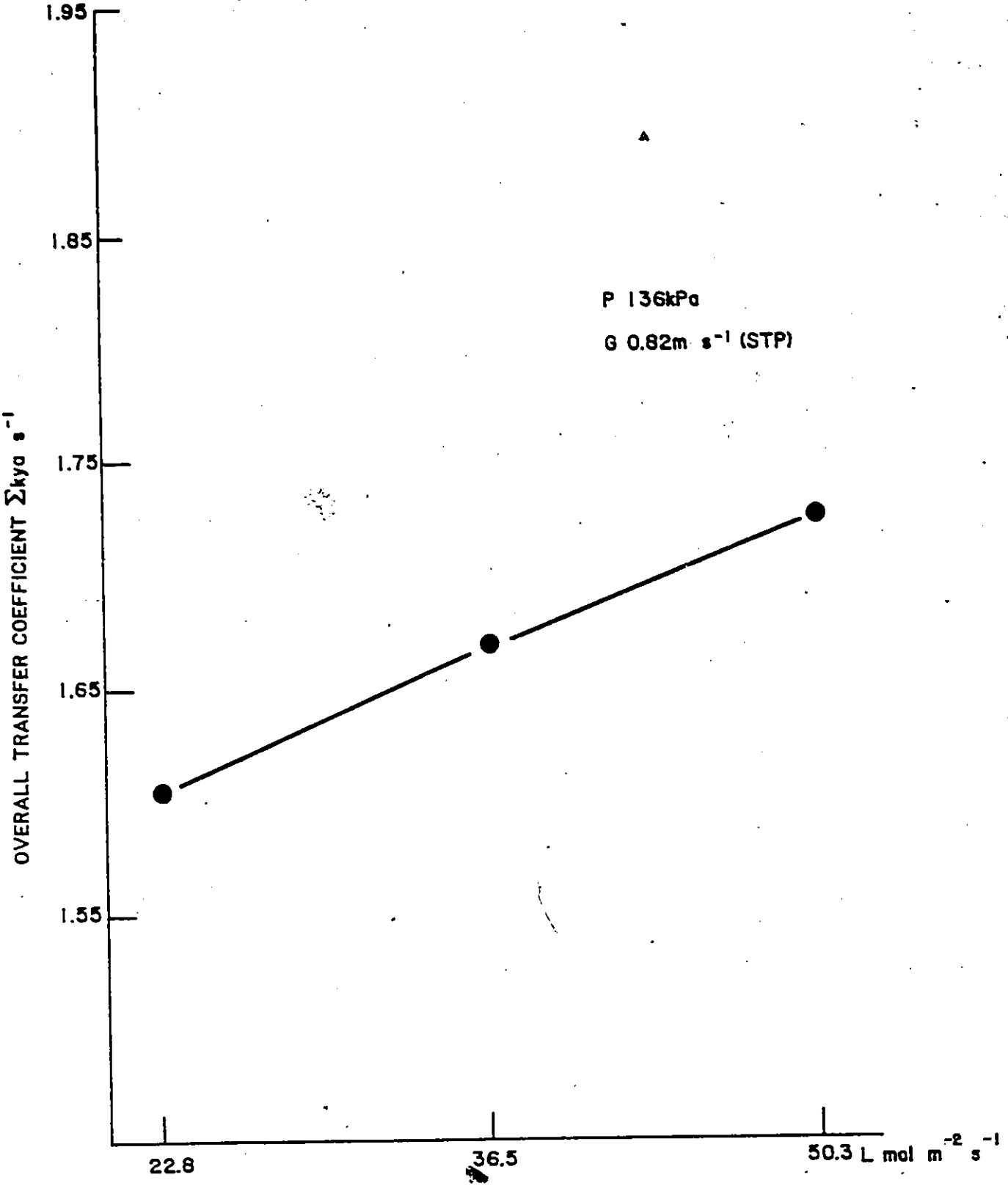

FIGURE 21 EFFECTS OF LIQUID FLOW RATE ON Σkya AT 60°C

The influence of the above operating variables on $\Sigma K_y a$ has been correlated empirically by the following equation based on least squares analysis.

$$\Sigma K_y a = 6.91 \times 10^{-1} + 2.02 \times 10^{-3}(L) + 8.70 \times 10^{-3}(G) - 9.13 \times 10^{-3}(P) \quad [39]$$

The significance of this correlation has been evaluated (see section 8.4).

4.5 Catalyst performance at 75°C and the effect of oxygen injection

After all the test runs at 60°C had been completed, the operating temperature was raised to 75°C. With the increase in temperature, the overall transfer coefficient $\Sigma K_y a$ also increased from 1.7 s^{-1} at 60°C to 2.3 s^{-1} at 75°C. Catalyst lifetime at 75°C is shown in Figure 22.

As can be seen from the figure, $\Sigma K_y a$ dropped to a steady state value of about 0.9 s^{-1} in 20 days of continuous operation. Since both hydrogen and water were purified to a great extent and no such decrease in activity was observed at 60 or 25°C, therefore, it was postulated that this low activity was probably due to significant water condensation inside the catalyst pores. Since the activity was comparable to those at 25°C (~0.7 s^{-1}), oxygen injection was initiated to test the possibility of recovering lost activity.

The optimum oxygen concentration at the gas inlet to the reactor was found to be 500 ppm above which no appreciable gain in activity was

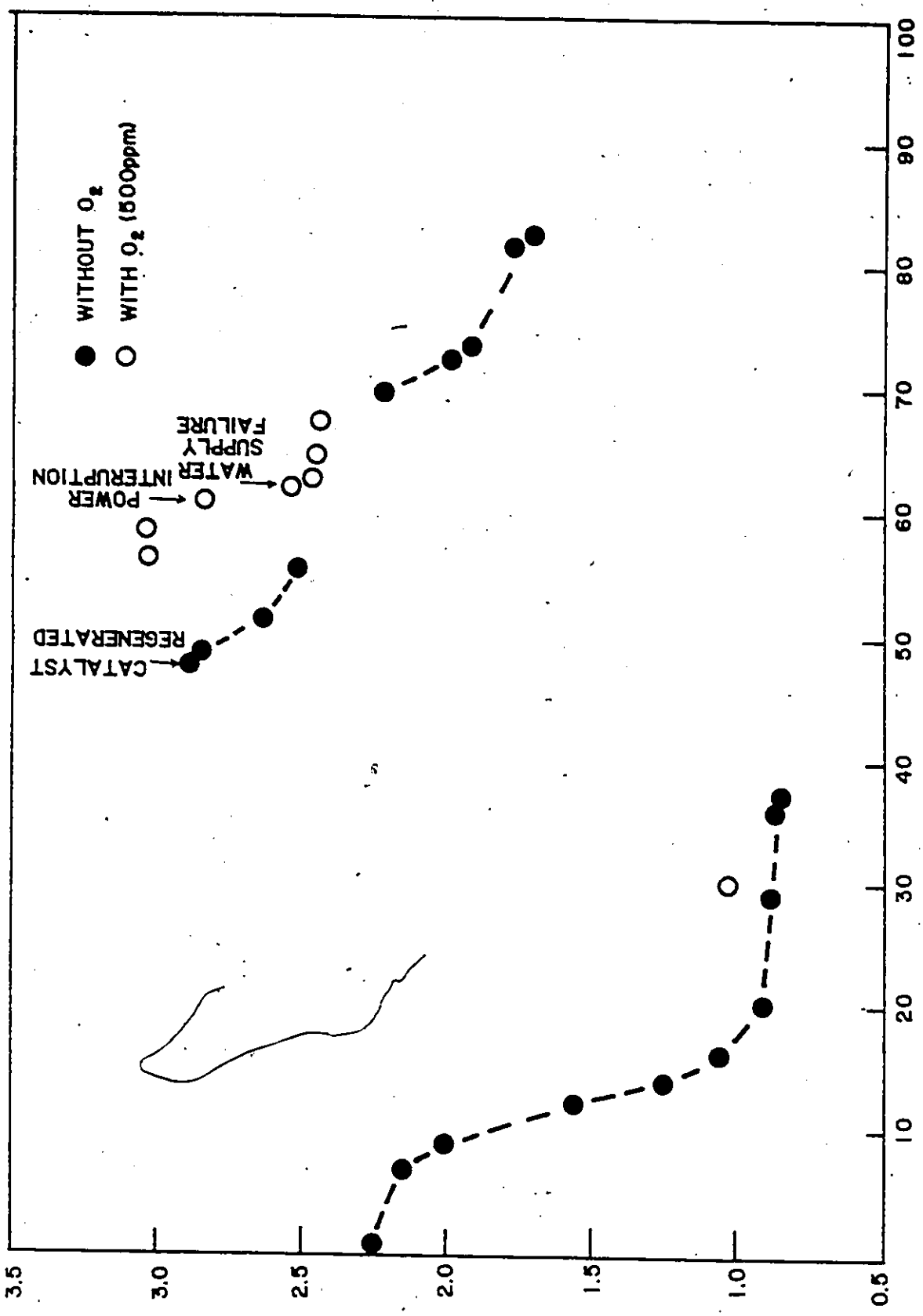

FIGURE 22 CATALYST LIFETIME AT 75°C AND THE EFFECT OF OXYGEN INJECTION

observed. Reactor temperature was monitored closely during oxygen injection, no detectable rise in temperature was measured and judging from both Japanese (12) and CRNL (21) reports, the bed height used in this study was unlikely to remove all the oxygen which should be available for reaction throughout the bed. With this oxygen level, $\Sigma K_y a$ was raised slightly from 0.8 to 1.0 s^{-1}. The activity did not recover to a higher level probably because the pores were already filled with condensed water which inhibited the fast catalyzed reaction between hydrogen and oxygen.

The catalyst was regenerated by passing hot air at about 120°C through the column and $\Sigma K_y a$ was found to be about 3 s^{-1}, and as expected, it again decreased with time. When $\Sigma K_y a$ decreased to 2.5 s^{-1} in 8 days of operation, oxygen was injected into the system and as a result $\Sigma K_y a$ increased back to about 3 s^{-1}. It stayed relatively constant for four days before it was interrupted by power failure and unscheduled shutdown of the building's distilled water supply. The corresponding ρk_R and ρk_D values at this level were about 70 and 140 $mol.m^{-3}.s^{-1}$, respectively.

After the two interruptions, $\Sigma K_y a$ dropped to 2.5 s^{-1}. Continuous injection of oxygen was able to maintain the activity at this level for seven days. To determine if the steady $\Sigma K_y a$ value was really due to the effect of oxygen injection, oxygen flow was discontinued and $\Sigma K_y a$ dropped from about 2.2 to 1.6 s^{-1} in 12 days of operation. The testing was discontinued due to the failure of the feed water pump. However,

the results at 75°C indicated that capillary water condensation could cause the catalyst to lose more than 60% of the original activity and oxygen injection into gas stream seemed to be able to avoid activity deterioration.

5. Conclusions

The catalyzed exchange of deuterium between hydrogen and water has been investigated in a trickle bed reactor under various operating conditions. The performance of the wetproofed catalyst may be divided into two categories, namely those at 60°C and those at 75°C.

At 60°C, the wetproofed catalyst can maintain long and stable activity. This substantiates the findings of other lifetime tests (10). The overall transfer coefficient increases with increasing gas and liquid flow whereas it decreases with rising system pressure. The influence of gas flow is relatively larger than those of liquid flow and system pressure indicating significant external diffusion resistance.

At 75°C, catalyst activity is reduced to that comparable to those at 25°C. It strongly suggests that this type of wetproofed catalyst can be deactivated by capillary condensation of water vapour in the pores of the catalyst. The results of oxygen injection indicated that continuous injection of 500 ppm of oxygen in the gas stream is effective in maintaining the activity but is incapable of restoring lost

activity. Lost activity can be recovered by flowing hot air at 120°C for four hours. However, this operation requires a shut down of the test facility.

6. Recommendations

1. The positive effects of oxygen injection at 75°C need to be established by testing for a longer period of time.

2. To avoid accidental addition of oxygen into hydrogen at concentration above the 6% explosion limit, other methods of introducing oxygen into the system should be investigated (e.g. the injection of H_2O_2 into the feed water has been proposed by K.T. Chuang).

3. For a given temperature and catalyst support, there will likely be some optimum pore size distribution with which to conduct hydrogen-water isotope exchange in a trickle bed reactor. This results from a compromise between total surface area and pore size distribution. However, for catalysts that are made of different support materials, the contact angle between water and the support is likely more important than the pore size distribution. Tests in these respects may provide information on catalysts that will retain most of their activity at temperatures close to the normal boiling point of water.

7. References

1. H.C. Urey, F.G. Brickwedde and G.M. Murphy, Phys. Rev., 39, p.164 (1932).

2. G.N. Lewis and R.T. MacDonald, J. Chem. Phys., 1, p.341 (1933).

3. J.A.L. Robertson, Science, 199, p.657 (1978).

4. W.P. Bebbington, V.R. Thayer and J.F. Proctor, "Production of heavy water Savannah River and Dana Plants", DP-400, The United States Atomic Energy Commission Contract AT(07-2)-1, (1959).

5. H.K. Rae, "Separation of Hydrogen Isotopes", American Chemical Society Symposium Series, 68, p.1 (1978).

6. G.M. Murphy, H.C. Urey and I. Kirshenbaum, "Production of heavy water", McGraw-Hill, New York, (1955).

7. J.T. Enright and T.T. Chuang, "Deuterium exchange between hydrogen and water in a trickle bed reactor", The Canadian Journal of Chemical Engineering, Vol. 56, p.246 (1978).

8. J.H. Rolston, "Research on the separation of hydrogen isotopes by catalytic exchange", Synthesis and Application of Isotopically Labelled Compounds Symposium, Kansas City, D.W. Duncan and A.B. Susan Editors, p.385 (1982).

9. J.P. Butler, "Hydrogen isotope separation by catalyzed exchange between hydrogen and liquid water", Separation Science and Technology, 15 (3), p.371 (1980).

10. J.P. Butler and J.H. Rolston, CRNL internal report, (1982).

11. Memo from K.T. Chuang to J.P. Butler, "A Possible Alternative for Wet-Proofing H_2/H_2O Exchange Catalyst", November 14, (1975).

12. A. Kitamoto, Y. Takashima and M. Shimizu, " Separation of Deuterium by H_2/H_2O Reaction with Hydrophobic Platinum-Catalyst", Proceedings of the Second World Congress of Chemical Engineering, Montreal p.375, (1981).

13. J.H. Rolston, J. den Hartog and J.P. Butler, "The Deuterium Isotope Separation Factor Between Hydrogen and Liquid Water", J. of Phys. Chem., 80, p.1064 (1976).

14. N. Palibruda, "Approach to the Theory of Separating Columns with Successive Exchange between Three Fluids", Z. Naturforschg, 21A, p.745, (1966).

15. W.H. Stevens, U.S. Patent 3,888,974 (1975).

16. W.A. Seddon, K.T. Chuang, W.J. Holtslander, and J.P Butler, "Wetproofed Catalyst: A New and Effective Solution for Hydrogen Isotope Separation and Hydrogen/Oxygen Recombination", to be

published in Energy Sources Technology Conference and Exhibition, New Orleans, (1984).

17. J.P. Butler, J.D. Hartog, J.W. Goodale and J.H. Rolston, "Separation of Rate Processes for Isotopic Exchange Between Hydrogen and Liquid Water in Packed Columns", Proceedings of the Sixth International Congress on Catalysts, London, (1976).

18. W.M. Thurston, M.W.D. James and R.W. Jones, "Operating Manual AECL-Micromass 602C Deuterium/Hydrogen Mass Spectrometer System", CRNL-1391, (1975).

19. J.P. Butler, J.H. Rolston and W.H. Stevens, "Separation of Hydrogen Isotopes - Novel Catalysts for Isotopic Exchange between Hydrogen and Liquid Water", American Chemical Society Symposium Series 68, p.93 (1978).

20. J.T. Enright and K.T. Chuang, CRNL Internal Report, (1976).

21. J.H. Rolston, CRNL Internal Report, (1981).

22. D.W. Bacon, "Collection and Interpretation of Industrial Data", Department of Chemical Engineering, Queen's University, Kingston, Ontario, Canada.

8. APPENDICES

8.1 Derivation of the deuterium mass balance differential equations across an incremental section of the trickle bed reactor.

Consider an infinitesimal column element of the trickle bed reactor:

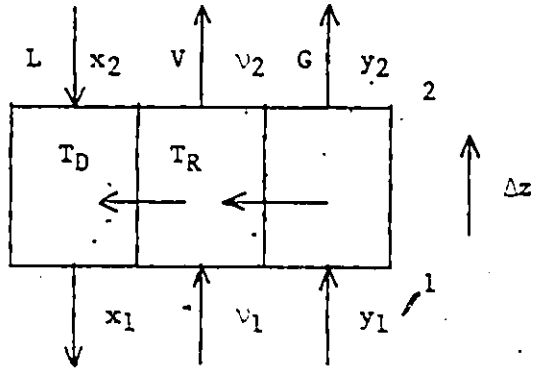

a) Detuerium atom mass balance in gas

$$-2G(y_2-y_1) = T_R\ \Delta z \qquad [40]$$

as $\Delta z \to o$

$$T_R = -2G\ \frac{dy}{dz} \qquad [41]$$

From the mechanism,

$$HD_G + H_2O_V \underset{k_2}{\overset{k_1}{\rightleftharpoons}} H_{2G} + HDO_V \qquad [42]$$

$$y \quad 1-\nu \qquad 1-y \quad \nu$$

$$T_R = k_1(y)(1-\nu) - k_2(1-y)(\nu) \quad [43]$$

$$T_R = k_2[\alpha_R\, y(1-\nu) - \nu(1-y)] \quad [44]$$

where $\alpha_R = k_1/k_2$

or $$T_R = \rho k_R'[\alpha_R\, y(1-\nu) - \nu(1-y)] \quad [45]$$

when ν and $y \ll 1$

$$T_R \simeq \rho k_R'(\alpha_R\, y - \nu) \quad [46]$$

Combining [41] and [46] gives

$$-2G \frac{dy}{dz} = \rho k_R'(\alpha_R\, y - \nu) \quad [47]$$

Let $$\frac{\rho k_R'}{2} = \rho k_R$$

$$\therefore \quad -G \frac{dy}{dz} = \rho k_R\, (\alpha_R\, y - \nu) \quad [48]$$

b) Deuterium atom mass balance in liquid water

$$-2L(x_2 - x_1) = T_D\, \Delta z \quad [49]$$

as $\Delta z \to 0$

$$T_D = -2L \frac{dx}{dz} \quad [50]$$

From the mechanism:

$$HDO_V + H_2O_L \underset{k_4}{\overset{k_3}{\rightleftharpoons}} H_2O_V + HDO_L \qquad [51]$$

$\nu \quad 1-x \qquad 1-\nu \quad x$

$$T_D = k_3\nu\,(1-x) - k_4\,x(1-\nu) \qquad [52]$$

or $$T_D = k_4[\alpha_D\,\nu(1-x) - x(1-\nu)] \qquad [53]$$

where $$\alpha_D = k_3/k_4$$

or $$T_D = \rho k_D'\,[\alpha_D\,\nu(1-x) - x(1-\nu)] \qquad [54]$$

when x and $\nu \ll 1$

$$T_D \simeq \rho k_D'\,(\alpha_D\nu - x) \qquad [55]$$

combining [50] and [55] gives,

$$-2L\,\frac{dx}{dz} = \rho k_D'\,(\alpha_D\nu - x) \qquad [56]$$

Let $$\frac{\rho k_D'}{2} = \rho k_D$$

$$\therefore \quad -L\,\frac{dx}{dz} = \rho k_D(\alpha_D\nu - x) \qquad [57]$$

c) Deuterium atom mass balance in water vapour

$$2V(\upsilon_2-\upsilon_1) = (T_R-T_D)\Delta z \qquad [58]$$

as $\Delta z \to o$

$$V\frac{d\upsilon}{dz} = -G\frac{dy}{dz} + L\frac{dx}{dz} \qquad [59]$$

8.2 Listing of program for the evaluation of transfer coefficients and a sample calculation.

```
      PROGRAM TWOPARM    74/74   OPT=1 ROUND=+-0/  PMDMP          FTN 4.8+498

      1               PROGRAM TWOPARM(INPUT,OUTPUT)
                C
                C     PROGRAM TO EVALUATE COLUMN PERFORMANCE IN TERMS OF
                C     VAPOUR-LIQUID TRANSFER COEFFICIENT
                C     GAS-VAPOUR TRANSFER COEFFICIENT
                C     AND OVERALL TRANSFER COEFFICIENT
                C
                      READ 1,DATE
                1     FORMAT (A10)
                2     FORMAT (1H1,3X,"DATE :",A10)
                      READ *,T,TP,VP,BH,RA,*,G,ET
                111   READ *,XI,YI,YO,YE
                      IF(XI.GT.1) GO TO 222
                      PRINT 2,DATE
                      XA=3.1416*RA**2/10000.
                      AF=A/(10.*50.*XA)
                      SH=G/(3600.*XA)
                      HF=SH*1000/22.413*
                      TPKPA=(14.7*TP)*6.89476
                      VPKPA=VP**2*2
                      HPKPA=TPKPA-VPKPA
                      M=VPKPA/HPKPA
                      VF=MS.M
                C
                C     CALCULATE SEPARATION FACTOR
                C
                      AK=EXP(-).2735+449.2/T+2350./T**2)
                      AD=EXP(3.3592-50.3/T+20490./T**2)
                      AL=AK*AD
                      ARE=EXP(-3.2735+449.2/ET+2350./ET**2)
                      VO=(YE*(1+ARE*M)-YO)/M
                      XO=(HF*YO+VF*VO-AF*XI-HF*YI)/(VF/AD-AF)
                      VI=XO/(AD*(1-XO)+XO)
                      YO=AK*YI
                C
                C     CALCULATE DRIVING FORCES AT TOP AND BOTTOM OF REACTOR
                C
                      DST=AR*YO-VO
                      DOT=AD*VO-XI
                      DSB=AR*YI-VI
                      DOB=AD*VI-XO
                      GAM=HF/(AF*AL-VF)
                      VOM=XI/AL
                      VOMA=XR*YO
                C
                C     CHECK FOR VALIDITY OF INPUT DATA
                C
                      IF(VO.LT.VOM) PRINT 10,VO,VOM
                10    FORMAT(1H0,4X,* VAPOR OUT = *,F9.7,* MIN VAPOR OUT = *,F9.7)
                      IF(VO.LT.VOM) STOP "BAD DATA "
                      EA=(VO-VOM)/(VOMA-VOM)
                      YOEL=XI/AL
                      YIEL=XO/AL
                      EFF=(YI-YO)/(YI-YOEL)
                      K=
                      J=
                      X=
```

```
PROGRAM TWOPARM    74/74   OPT=1 ROUND=*-*/  PMDMP          FTN 4.8+498

      C
      C     CALCULATE CONSTANTS REQUIRED FOR THE DETERMINATION OF
      C     TRANSFER COEFFICIENTS
      C
      7     RO=(OST-R)/(DOT+HF*R/(GAM*WF))*((HF+VF*AR)/WF-(HF*VF*(AR-GAM)
     $/(WF*WF*GAM))*(OST-R)/(DOT+(HF*OST/(GAM*WF))))
            O=(4*(HF/VF)*(RO/GAM)*(AR-GAM))/(AR+(HF/VF)*(1+RO/GAM))**2
            F=0.5*(AR+HF*(1+RO/GAM)/VF)*(1+SQRT(1-O))
            FF=0.5*(AR+HF*(1+RO/GAM)/VF)*(1-SQRT(1-O))
            AM=(ALOG((F*GAM*WF*OOB/HF)+(F-AR+GAM)*OSB)/((F-FF)
     $*(GAM*WF*)OOT/HF+OST)-(AR-GAM)*R)))/(FF*BH)
            D=(F-FF)*(AR-GAM)
            B=-FF*GAM*HF*(AO*VI-XO)/(D*HF)+(AR-GAM-FF)*(AR*YI-VI)/D
            RR=(F-FF)*B*EXP(-F*AM*BH)
            DIF=R-RR
            ADIF=ABS(DIF)
            IF(J.EQ.1) GO TO 4
            R1=R
            R2=RR
            OO=ADIF
            R=(R1+R2)/2.
            J=1
            GO TO 3
      4     CONTINUE
            IF(ADIF._LT.OO) GO TO 5
            R1=R
            GO TO 6
      5     CONTINUE
            R2=R
      6     CONTINUE
            R=(R1+R2)/2.
            GO TO 3
      3     CONTINUE
            N=N+1
            IF(N.GT.100) STOP " EXCESSIVE ITERATION "
            IF(ADIF._LT.OO) OO=ADIF
            IF(ADIF.GT.1.E-2) GO TO 7
            ROKR=AM*HF
            ROKO=RO*AM*WF
            A=(GAM/(AR-GAM))*(WF*XO-HF*YI-VF*VI)/HF
            C=(F*GAM*WF/(D*HF))*(AO*VI-XO)+(F-(AR-GAM))*(AR*YI-VI)/D
            VOA=AR*A+(AR-F)*B*EXP(-F*AM*BH)+(AR-FF)*C*EXP(-FF*AM*BH)
            YOA=A+B*EXP(-F*AM*BH)+C*EXP(-FF*AM*BH)
            TU=ALOG((YI-YIEL)/(YO-YOEL))
            OKYA=SH*(YI-YO)*TU/(BH*((YI-YIEL)-(YO-YOEL)))
      C
      C     PRINTING OF RESULTS
      C
            SKYAINV=(1/(AR*ROKR)+1./(AL*ROKO))*44.616E00
            SKYA=1/SKYAINV
            XOLM=(HF/WF)*(YI-YO)+XI
            YIEL=XO_M/AL
            TULM=ALOG((YI-YIEL)/(YO-YOEL))
            OKYALM=SH*(YI-YO)*TULM/(BH*((YI-YIEL)-(YO-YOEL)))
            PRINT 11,T,ET,TP,TPKPA,VP,VPKPA,BH,XA,W,WF,G,HF,SH,VF,XI
     $,XO,XOLM,VI,VO,YI,YO,YE,VOE,ROKR,ROKO,YOA,VOA
      11    FORMAT(1HO,/,5X,"COLUMN TEMPERATURE (K) =",F6.1,5X,
```

```
PROGRAM TWOPARM    74/74  OPT=1 ROUND=+-*/  PMDMP          FTN 4.8+498

     &"EQUILIBRATOR TEMPERATURE (K) =",F6.1,/,
     &1HO,4X,"TOTAL PRESSURE (PSIG) (KPA) =",F6.3,6X,F8.3,/,
     &1HO,4X,"VAPOUR PRESSURE (BAR) (KPA) =",F8.5,6X,F8.5,/,
     &1HO,4X,"BED HEIGHT (M) =",F6.3,6X,"AREA (M**2) =",F8.5,/,
     &1HO,4X,"WATER FLOW RATE (G/MIN) (MOL/MMS) =",F7.3,6X,F7.3,/,
     &1HO,4X,"GAS FLOW RATE (L/MIN) (MOL/MMS) (M/S) =",3F8.3,/,
     &1HO,4X,"VAPOUR FLOW RATE (MOL/MMS) =",F8.5,/,
     &1HO,4X,"WATER IN =",F9.7,6X,"WATER OUT =",F9.7,
     &2X,"WATER OUT LM =",F9.7,/,
     &1HO,4X,"VAPOUR IN =",F9.7,6X,"VAPOUR OUT =",F9.7,/,
     &1HO,4X,"GAS IN =",F9.7,6X,"GAS OUT =",F9.7,/,
     &1HO,4X,"EQUILIBRATOR (GAS OUT) =",F9.7,"  (VAPOUR OUT) =",F9.7,
     &1HO,4X,"CATALYTIC TRANSFER COEFFICIENT (MOL/MMMS) =",F8.3,/,
     &1HO,4X,"MASS TRANSFER COEFFICIENT (MOL/MMMS) =",F8.3,/,
     &1HO,4X,"ANALYTIC GAS OUT =",F10.6,6X,"VAP OUT =",F10.6)
      PRINT 12,3<YA
12    FORMAT(1HO,4X,*OVERALL TRANSFER COEFFICIENT KYA (1/S) =*,F7.3)
      PRINT 13,EFF
13    FORMAT(1HO,4X,*COLUMN EFFICIENCY =*,F8.5)
      PRINT 14,FA
14    FORMAT(1HO,4X,*FRACTIONAL LOCATION OF VAPOUR =*,F8.5)
      PRINT 15,3<YALM,SKYA
15    FORMAT(1HO,4X,"KYA MASS BALANCE (1/S) =",F7.3,/,
     &1HO,4X,"SIGMA KYA (1/S) =",F7.3)
      PRINT 16,AR,AD,AL,ARE,AD
16    FORMAT(1HO,4X,"ALR =",F7.3,2X,"ALD =",F7.3,2X,
     &"ALPHA =",F7.3,2X,"ALE =",F7.3,2X,"AD =",F7.3)
      GO TO 111
222   STOP
      END
```

Sample calculation of transfer coefficients:

Input data:

$G = 36.69$ mole.$m^{-2}.s^{-1}$

$L = 36.55$ mole.$m^{-2}.s^{-1}$

$V = 6.3$ mole.$m^{-2}.s^{-1}$

$T = 333$ K $\qquad Z = 0.4$ m

$\alpha_R = 2.9949 \qquad \alpha_D = 1.0491 \qquad \alpha = 3.1419$

$y_o = 355$ ppm $\qquad y = 200$ ppm

$x_o = 314$ ppm $\qquad x = 144$ ppm

$\nu_o = 299$ ppm $\qquad \nu = 216$ ppm

$\Delta R = \alpha_R\, y - \nu$

$= (2.9949)(200\times10^{-6}) - (216\times10^{-6})$

$= 3.83\times10^{-4}$

$\Delta_{Ro} = \alpha_R\, y_o - \nu_o$

$= (2.9949)(355\times10^{-6}) - (299\times10^{-6})$

$= 7.64\times10^{-4}$

$\Delta D = \alpha_D \nu - x$

$= (1.0491)(216\times10^{-6}) - (144\times10^{-6}) = 8.30\times10^{-5}$

$\Delta_{Do} = \alpha_D\, \nu_o - x_o$

$= (1.0491)(299\times10^{-6}) - (314\times10^{-6}) = 0$

$\gamma = G/(L\, \alpha_D - V)$

$= 36.69/[(36.55)(1.0491) - 6.30] = 1.14$

$$\phi = \frac{\Delta_R - R}{\Delta_D + (G/\gamma L)R}\left\{\frac{G+V\alpha_R}{L} - \frac{GV(\alpha_R-\gamma)}{L^2\gamma} \times \frac{\Delta_R - R}{\Delta_D + (G/\gamma L)\Delta_R}\right\}$$

$$R = (f_1 - f_2)B \, \mathrm{Exp}(-f_1\lambda z)$$

$$B = \frac{-f_2\gamma}{(f_1-f_2)(\alpha_R-\gamma)} \frac{L}{G}(\alpha_D\nu_o - x_o) + \frac{\alpha_R-\gamma-f_2}{(f_1-f_2)(\alpha_R-\gamma)}(\alpha_R y_o - \nu_o)$$

$$f_1 = \tfrac{1}{2}[\alpha_R + (G/V)(1+\phi/\gamma)](1+\sqrt{1-Q})$$

$$f_2 = \tfrac{1}{2}[\alpha_R + (G/V)(1+\phi/\gamma)](1-\sqrt{1-Q})$$

$$Q = \frac{4(G/V)(\phi/\gamma)(\alpha_R-\gamma)}{[\alpha_R + (G/V)(1+\phi/\gamma)^2}$$

Since ϕ is required in Q, therefore ϕ has to be obtained through successive approximations, starting with R = 0 for the first approximation of ϕ.

$$\phi = \frac{3.83\times10^{-4}}{8.30\times10^{-5}}\left\{\frac{36.69+6.30\ (2.9949)}{36.55} - \frac{(36.69)(6.30)(2.9949-1.14)}{(36.55)^2(1.14)} \times \frac{3.83\times10^{-4}}{(8.30\times10^{-5}) + (36.69)(3.83\times10^{-4})/(1.14)(36.55)}\right\}$$

$$= 5.83$$

$$\therefore Q = \frac{4(36.69/6.30)(5.83/1.14)(2.9949-1.14)}{[2.9949+(36.69/6.30)(1+5.83/1.14)]^2}$$

$$= 1.48\times10^{-1}$$

$$f_1 = \tfrac{1}{2}\left[2.9949 + \frac{36.69}{6.30}\left(1 + \frac{5.83}{1.14}\right)\right](1 + \sqrt{1-1.48\times10^{-1}})$$

$$= 36.95$$

$$f_2 = \tfrac{1}{2}\left[2.9949 + \frac{36.69}{6.30}\left(1 + \frac{5.83}{1.14}\right)\right](1 - \sqrt{1-1.48\times10^{-1}})$$

$$= 1.48$$

$$B = \frac{(-1.48)(1.14)}{(36.95-1.48)(2.9949-1.14)}\frac{36.55}{36.69}(1.0491)(299\times10^{-6})-(314\times10^{-6})$$

$$+ \frac{2.9949-1.14-1.48}{(36.95-1.48)(2.9949-1.14)}(7.64\times10^{-4})$$

$$= -4.28\times10^{-6}$$

$$\lambda = \frac{1}{f_2 z}\ln\frac{f_1(\gamma L/G)\Delta_{Do} + (f_1-\alpha_R+\gamma)\Delta_{Ro}}{(f_1-f_2)[(\gamma L/G)\Delta_D+\Delta_R] - (\alpha_R-\gamma)R}$$

$$= \frac{1}{(1.48)(0.4)}\times$$

$$\ln\frac{(36.95)(1.14)(36.55/36.69)(0)+(36.95-2.9949+1.14)(7.64\times10^{-4})}{(36.95-1.48)((1.14)(36.55/36.69)(8.30\times10^{-5})+3.83\times10^{-4})}$$

$$= 0.7757$$

$$R = (36.95-1.48)(4.28\times10^{-6})EXP[(-36.95)(0.7757)(0.4)]$$

$$= 1.5929\times10^{-9}$$

$$\sim 0$$

Therefore the first approximation of R=0 is reasonable.

$$\therefore \rho k_R = \lambda G$$

$$= (0.7757)(36.69)$$

$$= 28.5 \text{ mol.m}^{-3}.\text{s}^{-1}$$

$$\text{and } \rho k_D = \phi\lambda L$$

$$= (5.83)(0.7757)(36.55)$$

$$= 165 \text{ mol.m}^{-3}.\text{s}^{-1}$$

in terms of $\Sigma K_y a$,

$$\frac{i}{\Sigma K_y a} = \frac{44.616}{\alpha_o + x(1-\alpha_o)}\left[\frac{1+y(\alpha_R-1)}{\rho k_D} + \frac{\alpha_D + x(1-\alpha_D)}{\rho k_R}\right]$$

$$= \frac{44.616}{(3.1419)+(144\times10^{-6})(1-3.1419)}\left[\frac{1+200\times10^{-6}(2.9949-1)}{165} + \frac{(1.0491)+144\times10^{-6}(1-1.0491)}{28.5}\right]$$

$$\therefore \Sigma K_y a = 1.64 \text{ s}^{-1}$$

8.3 Derivation of the relation between ΣKy_a, ρk_R and ρk_D

Catalytic rate of the H_2/H_2O isotope exchange process can be described by:

$$0.5\ T_R = \rho\, k_R\ [\alpha_R y(1-\nu) - \nu(1-y)] \qquad [60]$$

and the mass transfer rate by,

$$0.5\ T_D = \rho\, k_D\ [\alpha_D \nu(1-x) - x(1-\nu)] \qquad [61]$$

The overall effect of the above two steps can be given by,

$$0.5\ T_o = \rho\, k_o\ (\alpha_o y(1-x) - x(1-y)) \qquad [62]$$

Equation [60] and [61] can be rewritten as,

$$0.5\ T_R = \frac{\rho k_R(1-\nu)}{\alpha_D(1-x)}\left[\frac{\alpha_R\alpha_D y(1-x)\ (1-\nu)}{(1-\nu)} - \frac{\alpha_D \nu(1-x)\ (1-y)}{(1-\nu)}\right] \qquad [63]$$

and

$$0.5\ T_D = \frac{\rho k_D(1-\nu)}{(1-y)}\left[\frac{\alpha_D \nu(1-x)\ (1-y)}{(1-\nu)} - \frac{x(1-\nu)\ (1-y)}{(1-\nu)}\right] \qquad [64]$$

the overall driving force term in [62] can be expanded as,

$$[\alpha_o y(1-x) - x(1-y)] = \left[\alpha_o y(1-x) - \frac{\alpha_D \nu(1-x)\ (1-y)}{(1-\nu)}\right] + \left[\frac{\alpha_D \nu(1-x)\ (1-y)}{(1-\nu)} - x(1-y)\right] \qquad [65]$$

Rearranging [62], [63] and [64] gives,

$$\frac{0.5\ T_o}{\rho k_o} = [\alpha_o y(1 - x) - x(1 - y)] \qquad [66]$$

$$\frac{0.5\ T_R \alpha_D (1 - x)}{\rho k_R (1 - \nu)} = \alpha_o y(1 - x) - \frac{\alpha_D \nu (1 - x)\ (1 - y)}{(1 - \nu)} \qquad [67]$$

and

$$\frac{0.5\ T_D (1 - y)}{\rho k_D (1 - \ )} = \frac{\alpha_D \nu (1 - x)\ (1 - y)}{(1 - \nu)} - x(1 - y) \qquad [68]$$

substituting [66], [67] and [68] into [65] yields,

$$\frac{T_o}{\rho k_o} = \frac{T_R \alpha_D (1 - x)}{\rho k_R (1 - \nu)} + \frac{T_D (1 - y)}{\rho k_D (1 - \nu)} \qquad [69]$$

At steady state, $T_o = T_R = T_D$

$$\therefore \frac{1}{\rho k_o} = \frac{\alpha_D (1 - x)}{\rho k_R (1 - \nu)} + \frac{(1 - y)}{\rho k_D (1 - \nu)} \qquad [70]$$

The overall transfer rate can also be defined as

$$0.5\ T_o = \Sigma K_y a' (y - y^*) \qquad [71]$$

therefore equating [62] and [71] and simplifying give,

$$\frac{1}{\rho k_o} = \frac{\alpha_o + x(1 - \alpha_o)}{44.617\ \Sigma K_y a} \qquad [72]$$

therefore equation [70] becomes

$$\frac{\alpha_o + x(1 - \alpha_o)}{44.617\ \Sigma K_y a} = \frac{\alpha_D(1 - x)}{\rho k_R(1 - \nu)} + \frac{(1 - y)}{\rho k_D(1 - \nu)} \qquad [73]$$

or

$$\frac{1}{\Sigma K_y a} = \frac{44.617}{[\alpha_o + x(1 - \alpha_o)]\ (1 - \nu)} \left[\frac{\alpha_D(1 - x)}{\rho k_R} + \frac{(1 - y)}{\rho k_D}\right] \qquad [74]$$

At steady state we can also write,

$$\rho k_R[\alpha_R y(1 - \nu) - \nu(1 - y)] = \rho k_D[\alpha_D \nu(1 - x) - x(1 - \nu)] \qquad [75]$$

Expand and express in terms of ν gives,

$$\nu = \frac{\rho k_R \alpha_R y + \rho k_D x}{\rho k_R(\alpha_R y + 1 - y) + \rho k_D[x + \alpha_D(1 - x)]} \qquad [76]$$

$$\therefore 1 - \nu = \frac{\rho k_R(1 - y) + \rho k_D \alpha_D(1 - x)}{\rho k_R[\alpha_R y + (1 - y)] + \rho k_D[x + \alpha_D(1 - x)]} \qquad [77]$$

put [77] into [74] gives,

$$\frac{1}{\Sigma K_y a} = \frac{44.617}{\alpha_o + x(1 - \alpha_o)} \left[\frac{\rho k_R(\alpha_R y + 1 - y) + \rho k_D[x + \alpha_D(1 - x)]}{\rho k_R(1 - y) + \rho k_D \alpha_D(1 - x)}\right] \qquad [78]$$

$$\left[\frac{\alpha_D(1 - x)}{\rho k_R} + \frac{(1 - y)}{\rho k_D}\right]$$

[78] can be simplified to give the final form of the relation between $\Sigma K_y a$, ρk_R and ρk_D.

$$\frac{1}{\Sigma K_y a} = \frac{44.617}{\alpha_o + x(1 - \alpha_o)} \left[\frac{1 + y(\alpha_R - 1)}{\rho k_D} + \frac{\alpha_D + x(1 - \alpha_D)}{\rho k_R} \right] \quad [79]$$

8.4 Evaluation of the correlation between $\Sigma K_y a$ and other operating variables.

The following data were used to obtain correlation:

L mol.m^{-2}.s^{-1}	G m.s^{-1}(STP)	P kPa	$\Sigma K_y a$ s^{-1}
36.5	0.82	163	1.648
36.5	0.82	108	1.721
36.5	0.62	136	1.481
36.5	1.03	136	1.916
22.8	0.82	136	1.604
50.3	0.82	136	1.725
36.5	0.82	136	1.683, 1.673, 1.679, 1.641, ...1.675

From the above data, the following correlation was obtained by least squares analysis.

$$\Sigma K_y a = 6.91 \times 10^{-1} + 8.70 \times 10^{-3}\, G + 2.02 \times 10^{-3}\, L - 9.12 \times 10^{-3}\, P \quad [80]$$

A 95% confidence interval for each of the estimated parameters is given below:

Estimated Least Squares Parameters	Lower Confidence Limit	Upper Confidence Limit
6.91×10^{-1}	5.27×10^{-1}	8.55×10^{-1}
8.70×10^{-3}	7.38×10^{-3}	1.00×10^{-2}
2.02×10^{-3}	9.21×10^{-4}	3.11×10^{-3}
-9.12×10^{-3}	-1.73×10^{-4}	-9.07×10^{-4}

The significance of the correlation inadequacy can be tested by comparing R with the value of $F_{\nu 1, \nu 2}$ (22).

$$R = \frac{\Sigma e_n^2 - \sigma^2 \nu_2}{\sigma^2} \qquad [81]$$

where Σe_n^2 sum of squares of residual

σ^2 estimated pure error variance

ν_2 degrees of freedom associated with σ^2

$$\Sigma e_n^2 = \sum_1^n (y_n - \hat{y}_n)^2 \qquad [82]$$

where

y_n response $\hat{y}_n$ estimated response

n number of data points

$$\sigma^2 = \sum_1^m (y_n - \bar{y})^2/(m-1) \qquad [83]$$

where $\bar{y} = (\sum_{1}^{m} y_n)/m$

m number of replicates

Substituting the appropriate values into the above equations gives

$$R = 5.62$$

From F distribution table F3, 4, 0.05 = 6.59.

Therefore, the comparison between R and F(3, 4, 0.05) suggests that any inadequacy in the fitted model is not significantly larger than experimental error. In addition, no trends were observed in the residual plot. Therefore the correlated equation is an adequate equation to represent the experimental data.

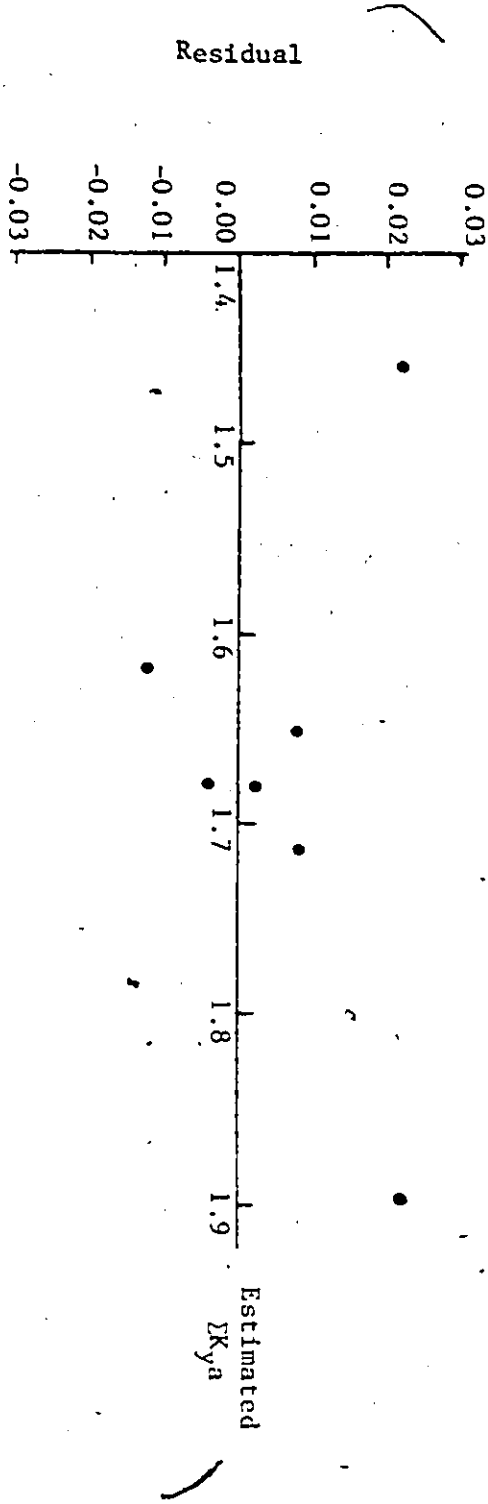

Figure 23: Residual plot for the experimental data

8.5 Equipment specification

1) Hydrogen purifier

Manufacturer:	Matheson
Model:	8374V
Capacity:	24 SLPM (50 SCFH)
Impurity level:	less than 0.5 ppm
Operating pressure:	345 to 1389 kPa

2) Rotameter for measuring recirculating hydrogen flow rate

Manufacturer:	Matheson
Model:	7640T, tube no. 605
Flow range:	stainless steel float 10-180 SLPM
	glass float 5-89 SLPM

3) Hydrogen mass flow controller

Manufacturer:	Tylan
Model:	FC260
Flow range:	0.06 to 3 SLPM
Accuracy:	±1% of full scale

4) Hydrogen flow meter

Manufacturer:	Tylan
Model:	FM362
Flow range:	0 to 150 SLPM
Accuracy:	±2% of full scale

5) Oxygen mass flow controller

Manufacturer:	Tylan
Model:	FC260
Flow range:	1 to 50 SCCPM
Accuracy:	±1% of full scale

6) Gas blower

Manufacturer:	Metal Bellows
Model:	MB-602 (explosion-proof motor)
Capacity:	57 SLPM at 172 kPa

7) Water purification system

Manufacturer:	Millipore
Model:	ZD20-115-74
Maximum flow:	1.5 SLPM

8) Recirculating water pump

Manufacturer:	Eastern
Model	2J34F
Capacity:	42 L PM at 207 kPa

9) Feed water rotameter

Manufacturer:	Matheson
Model:	7640T, tube no. 603
Flow range:	up to 133 cc/min

10) Spiking hydrogen gas rotameter

Manufacturer:	Matheson
Model:	7640T, tube no. 602
Flow range:	stainless steel float 80-2450 scc/min
	glass float 40-950 scc/min